

## Journal Pre-proofs

Design, synthesis and evaluation of the antibacterial activity of new Linezolid dipeptide-type analogues

G.D. García-Olaiz, Eleazar Alcántar-Zavala, Adrián Ochoa-Terán, Alberto Cabrera, Raquel Muñiz-Salazar, Julio Montes-Ávila, Alex J. Salazar-Medina, Efrain Alday-Noriega, Carlos Velazquez, José L. Medina-Franco, Rafael Laniado-Laborín

PII: S0045-2068(19)31375-6  
DOI: <https://doi.org/10.1016/j.bioorg.2019.103483>  
Reference: YBIOO 103483

To appear in: *Bioorganic Chemistry*

Received Date: 18 September 2019  
Revised Date: 22 November 2019  
Accepted Date: 25 November 2019

Please cite this article as: G.D. García-Olaiz, E. Alcántar-Zavala, A. Ochoa-Terán, A. Cabrera, R. Muñiz-Salazar, J. Montes-Ávila, A.J. Salazar-Medina, E. Alday-Noriega, C. Velazquez, J.L. Medina-Franco, R. Laniado-Laborín, Design, synthesis and evaluation of the antibacterial activity of new Linezolid dipeptide-type analogues, *Bioorganic Chemistry* (2019), doi: <https://doi.org/10.1016/j.bioorg.2019.103483>

This is a PDF file of an article that has undergone enhancements after acceptance, such as the addition of a cover page and metadata, and formatting for readability, but it is not yet the definitive version of record. This version will undergo additional copyediting, typesetting and review before it is published in its final form, but we are providing this version to give early visibility of the article. Please note that, during the production process, errors may be discovered which could affect the content, and all legal disclaimers that apply to the journal pertain.

© 2019 Published by Elsevier Inc.



## Design, synthesis and evaluation of the antibacterial activity of new Linezolid dipeptide-type analogues

G. D. García-Olaiz,<sup>1†</sup> Eleazar Alcántar-Zavala,<sup>1†</sup> Adrián Ochoa-Terán,<sup>1\*</sup> Alberto Cabrera,<sup>1</sup>  
Raquel Muñoz-Salazar,<sup>2</sup> Julio Montes-Ávila,<sup>3</sup> Alex J. Salazar-Medina,<sup>4</sup> Efrain Alday-  
Noriega,<sup>5</sup> Carlos Velazquez,<sup>5</sup> José L. Medina-Franco,<sup>6</sup> Rafael Laniado-Laborín,<sup>7,8</sup>

<sup>1</sup> Centro de Graduados e Investigación en Química, Tecnológico Nacional de México/Instituto Tecnológico de Tijuana. Tijuana, B. C. México.

<sup>2</sup> Laboratorio de Epidemiología y Ecología Molecular, Escuela Ciencias de la Salud, Universidad Autónoma de Baja California, Unidad Valle Dorado. Ensenada, B. C. México.

<sup>3</sup> Facultad de Ciencias Químico Biológicas, Universidad Autónoma de Sinaloa. Culiacán, Sin. México.

<sup>4</sup> Cátedras Conacyt - Departamento de Investigación en Polímeros y Materiales, Universidad de Sonora. Hermosillo, Sonora, México.

<sup>5</sup> Department of Chemistry-Biology, University of Sonora. Hermosillo, Sonora, México.

<sup>6</sup> Departamento de Farmacia, Facultad de Química, Universidad Nacional Autónoma de México. Ciudad de México, México.

<sup>7</sup> Clínica y Laboratorio de Tuberculosis, Hospital General de Tijuana, ISESALUD. Tijuana, B. C. México.

<sup>8</sup> Facultad de Medicina y Psicología, Universidad Autónoma de Baja California. Tijuana, B. C. México.

† These authors equally contribute to this work

\* Correspondence e-mail: [ochoa@tectijuana.mx](mailto:ochoa@tectijuana.mx)

## Abstract

Worldwide studies towards development of new drugs with a lower rate in emergence of bacterial resistance have been conducted. The molecular docking analysis gives a possibility to predict the activity of new compounds before to perform their synthesis. In this work, the molecular docking analysis of 64 Linezolid dipeptide-type analogues was performed to predict their activity. The most negative scores correspond to six Fmoc-protected analogues (**9as**, **9bs**, **9bu**, **10as**, **10ax** and **10ay**) where Fmoc group interacts in PTC for Linezolid. Twenty-six different Fmoc-protected Linezolid dipeptide-type analogues **9(as-bz)** and **10(as-bz)** were synthesized and tested in antimicrobial experiments. Compounds **9as**, **9ay**, **9ax**, **10as**, **10ay** and **9bu** show significant activity against group A *Streptococcus* clinical isolated. The analogue **10ay** also display high activity against ATCC 25923 *Staphylococcus aureus* strain and MRSA-3, MRSA-4 and MRSA-5 clinical isolates, with MIC values lower than Linezolid. The highest activity against multidrug-resistant clinical isolates of *Mycobacterium tuberculosis* was exhibited by **9bu**. Finally, a cytotoxicity assay with ARPE-19 human cells revealed a non-cytotoxic effect of **9bu** and **10ay** at 50 and 25  $\mu\text{M}$ , respectively.

**Keywords:** Linezolid analogues, dipeptide-type, docking, antibacterial activity, organic synthesis

## 1. - Introduction

The research of new antibiotics is essential due to the resistance developed by bacterial strains towards conventional antibiotics. The most important bacterial pathogens for humans evolved resistance and multi-resistance as result of a wide spread use of antibiotics through the last 70 years.<sup>1</sup> In United States, multi-resistant bacteria affect two million people per year, resulting in at least 23,000 dies per year.<sup>2</sup> Recently, World Health Organization (WHO) release a list of 12 antibiotic-resistant priority pathogens, such as *Staphylococcus aureus*, *Streptococcus pneumoniae* and *Mycobacterium tuberculosis*.<sup>3</sup> Oxazolidinones are a new group of antibiotics approved in 35 years.<sup>4</sup> Linezolid, an oxazolidinone based drug, is one of these outstanding therapeutic compounds with a different action mechanism (Figure 1).<sup>1,5</sup> Linezolid inhibits protein synthesis of bacterias in the initiation phase. An X-ray crystal

structure analysis showed its insertion in the 50S ribosome subunit through a hydrogen bond between the acetamidomethyl NH and phosphate of G2540 in the *Haloarcula marismortui* strain. In addition, an interaction between the C2487 and the fluorophenyl group is observed.<sup>6</sup>

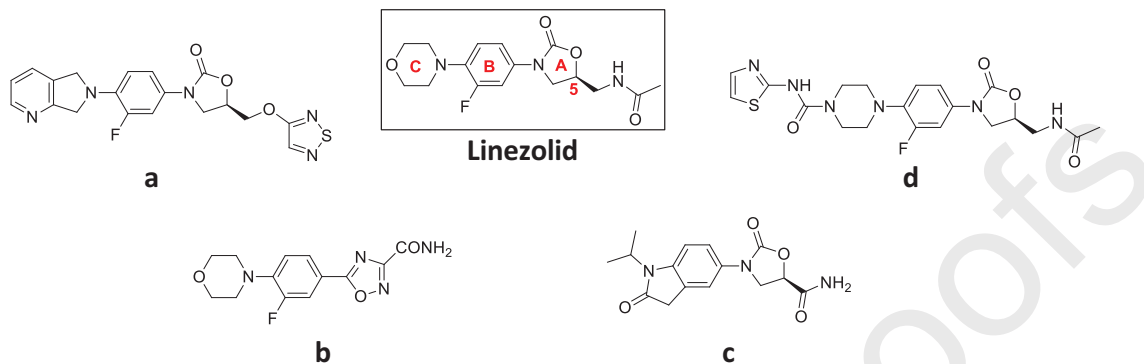


**Figure 1.** Chemical structure of Linezolid and different analogues modified in the C5 (a), A ring (b), B ring (c) and C ring (d).

Linezolid is active against most of Gram-positive bacteria and vancomycin-resistant enterococcus. However, there are current reports of resistance to Linezolid in *Staphylococcus epidermidis*, *Staphylococcus haemolyticus* and *Staphylococcus aureus* strains, especially in prolonged stay patients with nosocomial infections. Gram-positive bacteria usually develop resistance to Linezolid as result of mutation in G2576T, the Guanine base is replaced by Thymine in the 23S ribosome subunit.<sup>7,8</sup>

Since the emergence of resistant strains to inhibitory activity of Linezolid, structural analogues have been synthesized to improve its effectiveness.<sup>9-11</sup> The original structure has been modified in four sites: oxazolidinone (ring A)<sup>12</sup>, fluorophenyl group (ring B)<sup>13</sup>, morpholine (ring C)<sup>14</sup> and C5 substituent<sup>15</sup> (Figure 1). Structural modifications demonstrate that the presence of an *N*-aryl group is necessary to the biological activity, as well as, the *S* configuration at C5 in the oxazolidinone ring, which is essential to induce a positive influence in the antibacterial activity. Morpholine group provides a safe pharmacokinetic profile due to the presence of an electron donating group in the aromatic ring. Finally, the presence of a fluorine atom attached to an aromatic ring have shown to improve the antibacterial activity of Linezolid analogues.<sup>16-22</sup>

Nowadays, the design and development of new drugs are based on the benefits of low molecular weight drugs (less than 500 Da), which have conformational restriction, good membrane permeability, metabolic stability and oral bioavailability, combined with the selectivity in the action site and high potency of biological compounds (higher than 5000 Da).<sup>23</sup> The inclusion of peptide moieties in the structure of conventional drugs is an optimum strategy to improve their biological activity. These new compounds recognize as “peptide drugs” (structures with less than 50 amino acids) proved to be more active than their drug precursors.<sup>24</sup>

Pan *et. al.* synthesized dipeptide derivatives of dehydroabietic acid,<sup>24</sup> wherein the carboxylic group was modified with a dipeptide moiety showing a higher level of inhibitory activity against cancer cell lines, and a more potent effect than commercial anticancer drug 5-fluorouracil. Moreover, the structural inclusion of dipeptide moieties in conventional drugs has been develop in the antimicrobial area. These new antibiotics reduce bacterial resistance due to the rapid inhibition of bacterial growth by physical disruption of cell membranes.<sup>24</sup> The functional groups in a dipeptide moiety establish more interactions, resulting in an improved interaction in the action site.<sup>25</sup> Therefore, antibacterial activity of Linezolid may be enhanced including a dipeptide-type moiety to increase the number of interactions in the PTC. In fact, the enhanced antimicrobial activity of Tedizolid, a new Linezolid analogue drug, is attributed to its interaction in the action site through four-hydrogen bonds.<sup>26</sup>

Some Linezolid analogues have been synthesise modifying the C5 substituent with different amphiphilic segments such as amino acids (Lysine or Arginine), hydrophobic chains and cationic segments.<sup>27</sup> These analogues display activity against Gram-negative strains as *E. coli* and *S. enterica* with MIC values of 8 µg/mL (Linezolid was 64 µg/mL). However, these compounds were inactive in a serum-blood (1:1) solution. This result is due to presence of negative charges in proteins and other macromolecules present in serum and blood, which bind to cationic molecules, and avoid their transport into bacterial membrane. Some thiazolidinone dipeptide type analogues have been synthesized and tested as inhibitors of type III secretion system in *Salmonella enterica* serovar *Typhimurium*. The IC<sub>50</sub> obtained for the most analogues modified as dipeptides, were lower than the obtained with the thiazolidinone precursor.<sup>28</sup>

Previously, we reported the diastereoselective synthesis of ten dibenzylamino oxazolidinones by chemical modification of five different  $\alpha$ -aminoacids.<sup>29</sup> The *in vitro* antibacterial assays were performed with 12-methicillin resistant *Staphylococcus aureus* clinical isolates. The oxazolidinone derived of L-alanine exhibited antibacterial activity in the Kirby-Bauer diffusion susceptibility protocol at 6.6  $\mu\text{g}$  and a MIC value of 12.5  $\mu\text{g}/\text{mL}$  in the microdilution method.<sup>30</sup>

Here we report the molecular docking and antibacterial activity of Linezolid dipeptide-type analogues, which preserve A, B and C rings of Linezolid, with a variation in A ring configuration (*R* or *S*) (Figure 2). The construction of A ring is achieved by chemical modification of L-Alanine ( $R_1$ = methyl) and L-Phenylalanine ( $R_1$ = benzyl), leading to oxazolidinone diastereomers (*S,R* and *S,S*).<sup>31</sup> The combinatorial coupling with a Fmoc-protected amino acid (AA) leads to *S,R,S* and *S,S,S* diastereomers. L-Alanine and L-Phenylalanine were chosen to build the A ring considering the antibacterial activity of the oxazolidinone derivative,<sup>30</sup> and to evaluate the effect of an aromatic ring in the molecular coupling and antibacterial activity. The amino acids selected as AA have different structural characteristics such as aromatic and heteroaromatic rings (Phe, Trp, His, Tyr), aliphatic (Leu) and heteroaliphatic (Thr, Cys, Ser) groups, further, the protective group is Fmoc. The combination of the four-diastereomeric oxazolidinones with the AA<sub>2</sub> amino acids leads to 32 compounds. The total deprotection of these compounds finally reached a database of 64 Linezolid dipeptide-type analogues for testing in the molecular docking analysis.

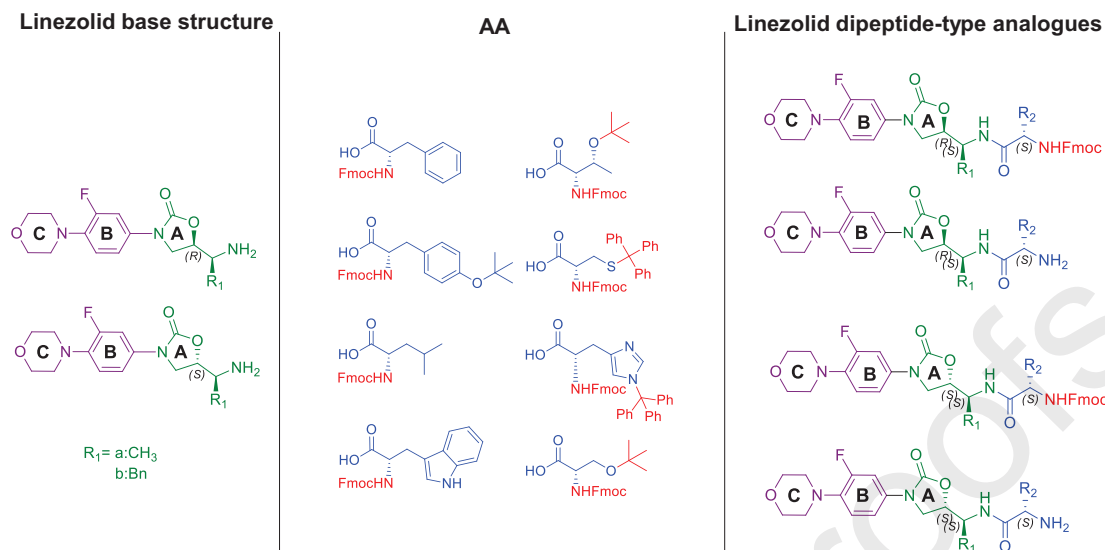


**Figure 2.** Combinatorial strategy to design the Linezolid dipeptide-type analogues.

The hypothesis of this study lays in structural modifications of Linezolid with  $\alpha$ -amino acids to maintain or increase of their activity, as well as, retard the bacterial resistance. These Linezolid dipeptide-type analogues have the amide group required to establish a typical hydrogen bond interaction, and different  $R_1$  and  $R_2$  groups, which may display different interactions in the action site.

### 3. – Results and discussion

#### 3.1 Molecular docking studies

The molecular docking of Linezolid and analogues was performed into the crystallographic structure of ribosomal RNA (rRNA) of *E. coli*. The crystallographic structure was reported at 3.5 Å of resolution for Schuwirth *et al.*<sup>32</sup> The Phosphoryl Transferase Center (PTC) in 4V4Q is located in the *E. coli* 23S rRNA subunit. The binding pocket is made up of a group of nucleotides within of 4.5 Å in relation with the atoms of the ligand. This structure was selected to perform the molecular docking deleting ligands such as magnesium ion, water molecules, ribosomal proteins and a repetitive chain of rRNA.

The geometry of molecules was optimized with the QuickPrep application implemented in MOE program,<sup>33</sup> which adds hydrogen and establishes protonation states, fixes distant atoms of receptor from the molecule, and leaves free nearby atoms. First, the molecular docking of Linezolid was performed considering flexible the atoms of molecule and receptor. An AMBER force field (AMBER10:EHT) was selected to produce an homogeneous distribution of the low energy conformations (500 interactions in total with 30 consecutive attempts to find a better solution) and the best coupling result was selected.<sup>34</sup>

Molecular docking of Linezolid with MOE program shows a hydrogen bond interaction with G2505. In the boundaries of PTC are G2505 and U2506 surrounding the guest near to oxazolidinone ring, as was observed in docking with Linezolid by Shaw *et al.*<sup>26</sup> More nucleotides that surround the guest are A2503, A2451 and C2452. However, an opposite orientation of fluorine atom was found in our model (Figure S1). The coupling score value is -7.21 kcal/mol and a *redocking* give a RMSD value of 1.17 Å. A second Linezolid molecular docking was performed with LEDOCK 2018 program,<sup>35</sup> in order to verify the consistency and reproducibility of the pose reported by MOE 2018. As depicted in Figure S2, this analysis predicted a similar pose than MOE and there is perfect overlap of both poses obtained by the two programs. The score value obtained by LEDOCK program was -6.02 kcal/mol. The different orientation of fluorine atom in our model is presumably due to the refinement in the programs algorithms looking for predictions that are more accurate and the use of a different crystal structure of the rRNA for *E. coli*.

Once the molecular docking of Linezolid was validated with MOE and LEDOCK, the molecular docking of 64-Linezolid dipeptide-type analogues was performed into the crystallographic structure of rRNA in MOE 2018. The analysis showed 30 guests occupying the PTC and showing a hydrogen bond interaction between amide group of Linezolid and the G2505 nucleotide of the rRNA fragment. Noteworthy, the most negative scores (in kcal/mol) correspond to the six protected analogues (**9as**, **9bs**, **9bu**, **10as**, **10ax** and **10ay**) where the Fmoc and the other protecting groups interacting in PTC (Table 1). The score value obtained after several calculations is related to the quality of the coupling, where the lower scores indicate the most favorable couplings. Based on the docking results and a previous report of antibacterial activity in *E. coli* and *S. aureus* strains and docking studies of *N*-protected

(Fmoc-protected) hydroxyamic acids,<sup>36</sup> this research was focused in the study of the Linezolid dipeptide-type analogues bearing non-polar protecting groups.

**Table 1.** Score of the molecular coupling experiment.

Compound	Diastereomer	R <sub>1</sub>	AA	Score (kcal/mol)
<b>9as</b>	<i>R,S,S</i>	CH <sub>3</sub>	Phe	-10.42
<b>10as</b>	<i>S,S,S</i>	CH <sub>3</sub>	Phe	-9.41
<b>9bu</b>	<i>R,S,S</i>	Bn	Leu	-9.38
<b>9bs</b>	<i>R,S,S</i>	Bn	Phe	-10.23
<b>9ax</b>	<i>R,S,S</i>	CH <sub>3</sub>	Cys	-9.85
<b>10ay</b>	<i>S,S,S</i>	CH <sub>3</sub>	Hys	-10.67
<b>Linezolid</b>				-7.21

Standard deviation  $\pm 1.05$

Average -8.4289

The docking of analogue **9as** (green color) in PTC is an example of a perfect superposition with Linezolid (yellow color). This guest establish a typical hydrogen bond of amide NH with G2505, similar to Linezolid. In addition, there is a  $\sigma$ - $\pi$  interaction between the fluorene ring (Fmoc group) and hydrogen in C<sub>2</sub> of the purine in A2062 (Figure 3).

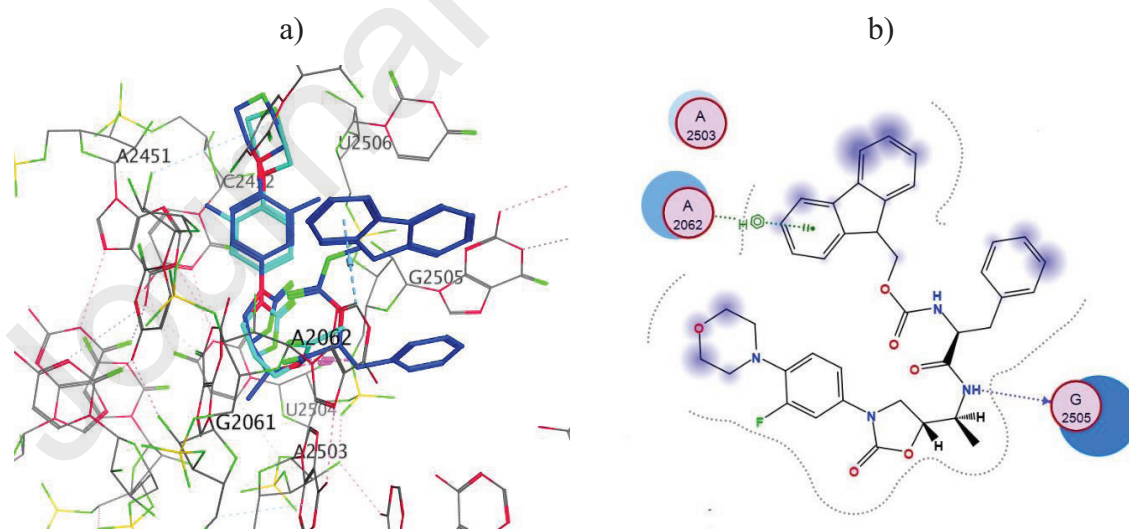


**Figure 3.** a) Molecular docking of **9as** (blue) and Linezolid (magenta) in PTC and b) interactions map of **9as**.

Some analogues as **9bu** present a non-Linezolid like space arrangement, but they display more main interactions in PTC (Figure 4). Figure 4 shows the molecular docking of **9bu**, a  $\pi$ - $\pi$  interaction between the benzyl group and A2451 nucleotide base, a  $\sigma$ - $\pi$  interaction between Fmoc group and the G2505 nucleotide base and two additional hydrogen bond interactions with the same nucleotide are observed.

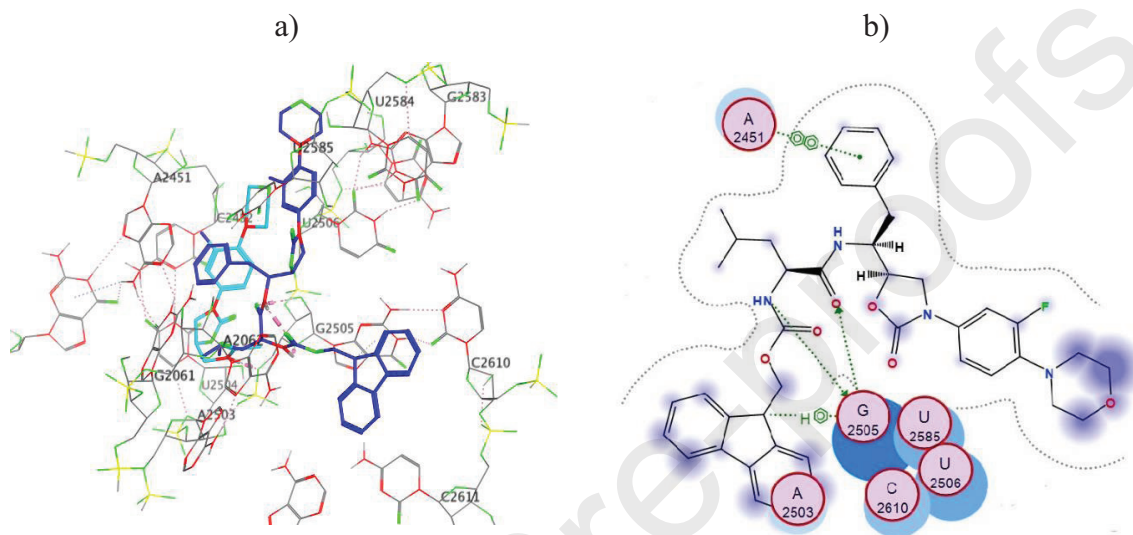


**Figure 4.** a) Molecular docking of **9bu** (blue) and Linezolid (magenta) in PTC and b) interactions map of **9bu**.

Analogue **10ay** presents a Linezolid shifted pose (yellow color) in the active site, and the characteristic hydrogen bond between amide NH and G2505 is not observed. The structure of **10ay** (yellow color) shows different interactions with G2061 and G2505 nucleotides in the molecular docking analysis. Apparently, there is a hydrogen bond with the Fmoc methylene group and a  $\pi$ - $\pi$  interaction with the imidazole and G2505 nucleotide. Additionally, a hydrogen bond interaction was observed between the carbonyl of the A ring and G2061 nucleotide (Figure 5).

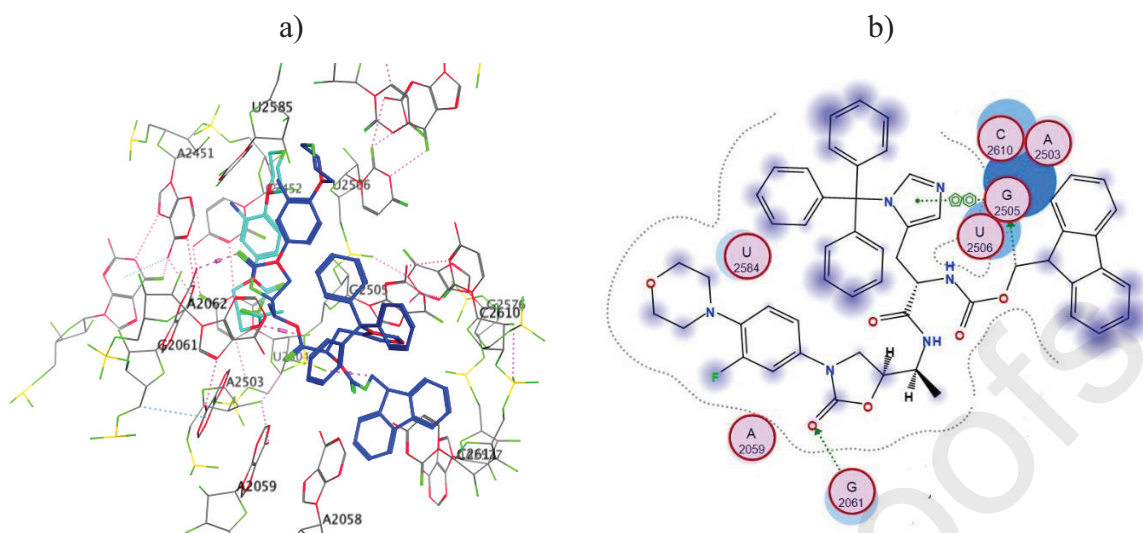


**Figure 5.** a) Molecular docking of **10ay** (blue) and Linezolid (magenta) in PTC and b) interactions map.

The molecular docking of the non-protected **10ay** analogue shows a shifted Linezolid-like pose (Figure 6). The hydrogen bond between the amide NH group of Linezolid and the G2505 phosphodiester is not present either, but the interaction of the G2061 nucleotide and the A ring carbonyl acting as hydrogen acceptor remains present. Noteworthy, the  $\pi$ - $\pi$  interaction of the unprotected imidazole ring with the guanine in the G2505 nucleotide is no longer present and two new hydrogen bond interactions between the amide carbonyl and free amine of the histidine with the G2505 nucleotide are established. The score value of these unprotected analogue is  $-7.93$  kcal/mol, which also predict a favorable activity.

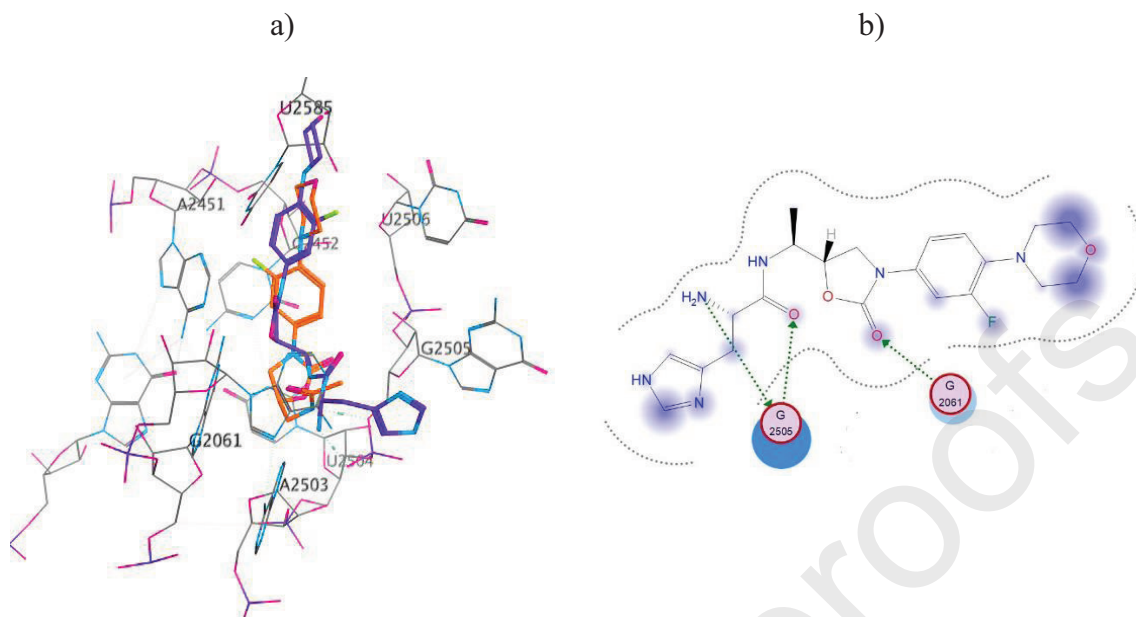
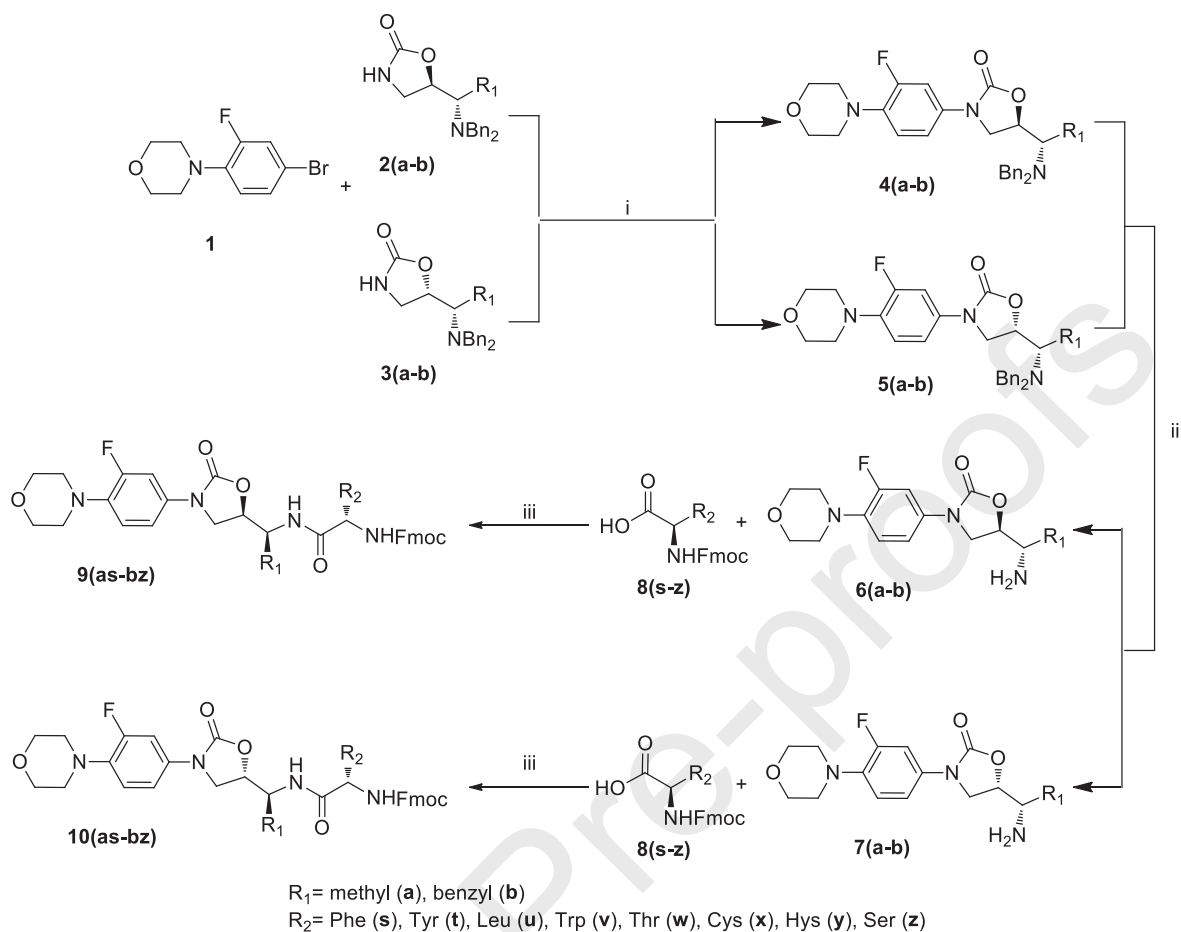


**Figure 6.** a) Molecular docking of non-protected **10ay** analogue (purple) and Linezolid (yellow) in PTC and b) interactions map.

In summary, the docking analysis of the Linezolid-dipeptide type analogues predicts additional interactions that favor their coupling in the PTC with score values thermodynamically more favorable. The protecting groups influence significantly in the spatial arrangement and in the nature and number of interactions in the PTC.

### 3.2 Chemistry

A library of 26 Linezolid dipeptide-type analogues was prepared following a three step syntheses pathway as depicted in Scheme 1. First, the chemical modification of L-alanine (**a**) and L-phenylalanine (**b**) leads to the diastereomeric oxazolidinone pair *S,R*-**2** and *S,S*-**3** from each amino acid, respectively (Scheme S1).<sup>29,30</sup> A *N*-aryl coupling was achieved with **1**<sup>31,37</sup> and **2(a-b)** and **3(a-b)**, respectively, using potassium carbonate, *N,N*-dimethylethylamine and copper iodide to obtain **4(a-b)** and **5(a-b)** in good yields. The hydrogenolysis of these intermediates was carried out with H<sub>2</sub>, Pd/C in methanol to give **6(a-b)** and **7(a-b)**. Finally, amine intermediates were reacted with Fmoc-protected amino acids **8(s-z)** (L-Phe, L-Leu, L-Tyr, L-Thr, L-Trp and L-Ser) using *N,N*-disopropylcarbodiimide (DIC) and 1-Hydroxybenzotriazole (HOBT) in DMF.



**Scheme 1.** Reagents and conditions: (i) CuI,  $K_2CO_3$ ,  $MeNH(CH_2)NHMe$ , Toluene,  $115^\circ C$ , 72 h; (ii)  $H_2$ , Pd/C 10%, MeOH, AcOH, 4 h; (iii) DIC, HOBT, DMF, 12 h.

The  $^1H$  NMR spectra of the oxazolidinones **2** and **3** show the signals for a  $A_2B_2C$  aromatic system at 7.36, 7.26 and 7.16 ppm and two doublets at 3.70 and 3.44 ppm due to presence of the dibenzyl amino protected group. There is a broad singlet at 6.45 ppm corresponding to the oxazolidinone N-H group and at 3.55 and 3.22 ppm are present the two signals for the diastereotopic methylene hydrogens. The signal of the stereocenter derived from de amino acid is observed at 4.46 ppm. The  $^{13}C$  NMR spectra show a signal for the carbonyl at 160.4 ppm, and at 79.9 and 44.8 ppm two signals assigned to the methine and methylene carbons of the oxazolidinone, respectively. All these signals evidence the presence of the oxazolidinone ring in their chemical structure. The signals corresponding the  $R_1$  substituent are also present. In addition, slight differences in the chemical shifts for some of

the signals in **2** and **3** confirm their different configuration (Figures S3-S10).<sup>29,30,38-41</sup> The FTIR spectra shows the vibration for the carbonyl in  $1733\text{ cm}^{-1}$  (Figure S13).

The  $^1\text{H}$  NMR spectrum of **1** shows a multiplet signal at 7.21 ppm and a double of doublets at 6.82 ppm assigned to aromatic hydrogens. Signals at 3.87 and 3.07 ppm corresponds to morpholine hydrogens. In the  $^{13}\text{C}$  NMR spectrum a doublet at 155.5 ppm with a  $J_{\text{C-F}} = 249.3$  Hz is assigned to the *ipso* fluorine carbon. A doublet at 113.9 ppm with  $J = 8.7$  Hz corresponds to the *ipso* bromine carbon. Finally, two signals at 66.9 and 50.8 ppm correspond to morpholine methylenes (Figures S11 and S12).

The  $^1\text{H}$  NMR spectra of **4** and **5** show signals corresponding to both precursors, with exception of the N-H signal at 6.45 ppm (Figures S16-S23). The presence of three signals at 7.20, 7.00 and 6.91 ppm corresponding to fluorophenyl group, two multiplet signals at 3.86 and 3.05 ppm assigned to morpholine hydrogens and signals for two diastereotopic hydrogens present in oxazolidinone at 3.82 and 3.57 ppm, confirm the presence of both fragments in these molecules. In the  $^{13}\text{C}$  NMR spectra is present the oxazolidinone carbonyl signal at 154.2 ppm, and a doublet at 155.5 ppm with  $J_{\text{C-F}} = 244.5$  Hz for the *ipso* fluorine carbon. The *ipso* amine carbon shifts to 136.3 ppm due to the bonding with nitrogen. These and the rest of signals confirm the two fragments coupling. In the FT-IR spectrum, a carbonyl vibration is present at  $1748\text{ cm}^{-1}$  (Figure S14).

The signals corresponding to benzylic groups are no longer observed in NMR spectra of **6** and **7**. A broad singlet at 4.31 ppm in  $^1\text{H}$  NMR spectra and a shift of the CH-N carbon from 56.8 to 48.3 ppm indicate the presence of a free amino group in these molecules (Figures S24 to S31).

Linezolid dipeptide-type analogues **9(as-bz)** and **10(as-bz)** display stretching vibration bands at  $1775\text{ cm}^{-1}$ ,  $1760\text{ cm}^{-1}$  and  $1684\text{ cm}^{-1}$  in their FTIR spectra, corresponding to Fmoc, oxazolidinone and amide carbonyls (Figure S15).  $^1\text{H}$  NMR spectra show two broad singlets at 6.30 and 5.45 ppm assigned to carbamate and amide hydrogens, respectively. A signal at 172 ppm corresponds to amide carbonyl and two signals at 154 ppm to carbamate and oxazolidinone carbonyls. These spectroscopic data evidence the formation of dipeptide analogues. Two-dimensional HSQC experiment were performed with these compounds, in

order to assign the rest of signals. NMR spectra (Figures S32 to S95) and total signal assignment are provided in the supplementary material (Tables S1 to S12).

### 3.3 Antibacterial activity against *Streptococcus* and *Staphylococcus* clinical strains.

The antibacterial efficacy of Linezolid dipeptide type analogues was determined by a microdilution assay and expressed as the minimum inhibitory concentration (MIC).<sup>44-46</sup> The compounds **9as**, **9ay**, **9ax**, **10as**, **10ay**, ( $R_1=CH_3$ ) and **9bu** ( $R_1=Bn$ ) showed significant activities (MIC of 3.125 to 25  $\mu\text{g/mL}$ ) against group A *Streptococcus* clinical isolate (Figure 7).

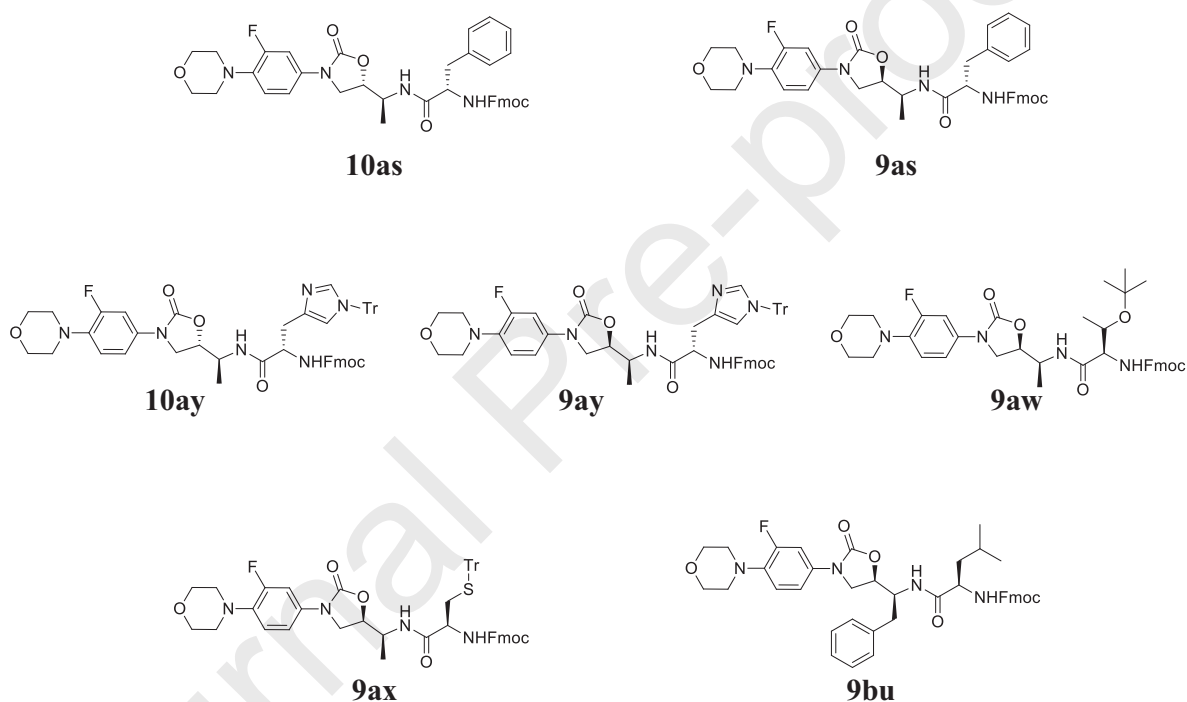


**Figure 7.** Active Linezolid dipeptide-type analogues against *Streptococcus* and *Staphylococcus* clinical strains.

There are more active analogues from L-alanine than L-phenylalanine (Table 2). However, none of these show more potency than Linezolid (0.5  $\mu\text{g/mL}$ ) against group A *Streptococcus* clinical strain. Interestingly, almost all active compounds have a *R,S,S* configuration, but the most active compound **10ay** is *S,S,S*, being twice more active than **9ay**. This result indicates that stereochemistry influences the antibacterial activity of Linezolid analogues.

**Table 2.** MICs of the Linezolid peptide-type analogues against drug-sensitive group A *Streptococcus* clinical strain (MIC:  $\mu\text{g/mL}$ ).

Compound	Diastereomer	R <sub>1</sub>	AA	MIC
<b>9as</b>	<i>R,S,S</i>	CH <sub>3</sub>	Phe	25.0
<b>9aw</b>	<i>R,S,S</i>	CH <sub>3</sub>	Thr	6.25
<b>9ax</b>	<i>R,S,S</i>	CH <sub>3</sub>	Cys	6.25
<b>9ay</b>	<i>R,S,S</i>	CH <sub>3</sub>	His	6.25
<b>9bu</b>	<i>R,S,S</i>	Bn	Leu	25.0
<b>10as</b>	<i>S,S,S</i>	CH <sub>3</sub>	Phe	25.0
<b>10ay</b>	<i>S,S,S</i>	CH <sub>3</sub>	His	3.125
<b>Linezolid</b>				0.5

The analogue **10ay** exhibits the highest activity against group A *Streptococcus* clinical strain among other analogues, and it is active against ATCC 25923 *Staphylococcus aureus* strain and MRSA-3, MRSA-4 and MRSA-5 clinical isolates, displaying lower MIC values than Linezolid (Table 3). The effect of compound **10ay** was determined by seeding the well content in which the MIC value was determined in TSA medium and incubated for 20 h. The bacterial growth in culture media shows **10ay** as bacteriostatic similar to Linezolid.

**Table 3.** Evaluation of the antibacterial activity of **10ay** against ATCC and clinical strains (MIC:  $\mu\text{g/mL}$ ).

Compound	ATCC 25923	MRSA-3	MRSA-4	MRSA-5	1
<b>10ay</b>	3.125	3.125	3.125	6.25	3.125
<b>Linezolid</b>	4	4	8	8	0.5

*Staphylococcus aureus* ATCC 25923. Clinical isolates of Meticilin Resistant *Staphylococcus aureus* met icilin resistant clinical strains (MRSA-3, MRSA-4, MRSA-5), group A *Streptococcus* (1).

Noteworthy, analogue **10ay** shows the best score value in the molecular docking analysis, as well as, performance in the antibacterial assay. The molecule of **10ay** presents three main interactions in the action site (Figure 4), while molecular docking of **9ay** shows two hydrogen bonding interactions with A2062 and G2505 (Figure S94). Both molecules

**9ay** and **10ay** occupy the PTC of Linezolid (Figure 8a), but a different configuration in C<sub>5</sub> of A ring leads to a different spatial arrangement, as well as, number and type of supramolecular interactions (Figure 8b). In **10ay** the imidazole ring establishes a  $\pi$ - $\pi$  interaction with G2505 and Fmoc group participates with two additional interactions. Analogue **9ay** establishes a hydrogen bond with imidazole ring, acting as acceptor and G2505 as donor, while the interaction with Fmoc group is not present. The analogues **9ax** and **9aw** have significant antibacterial activity consistent with their molecular docking analysis. The main interactions of these guests into the Linezolid PTC are  $\pi$ - $\pi$  and  $\sigma$ - $\pi$  interactions between Fmoc group and G2505, as well as, hydrogen bonding (Figures S97 and S98).

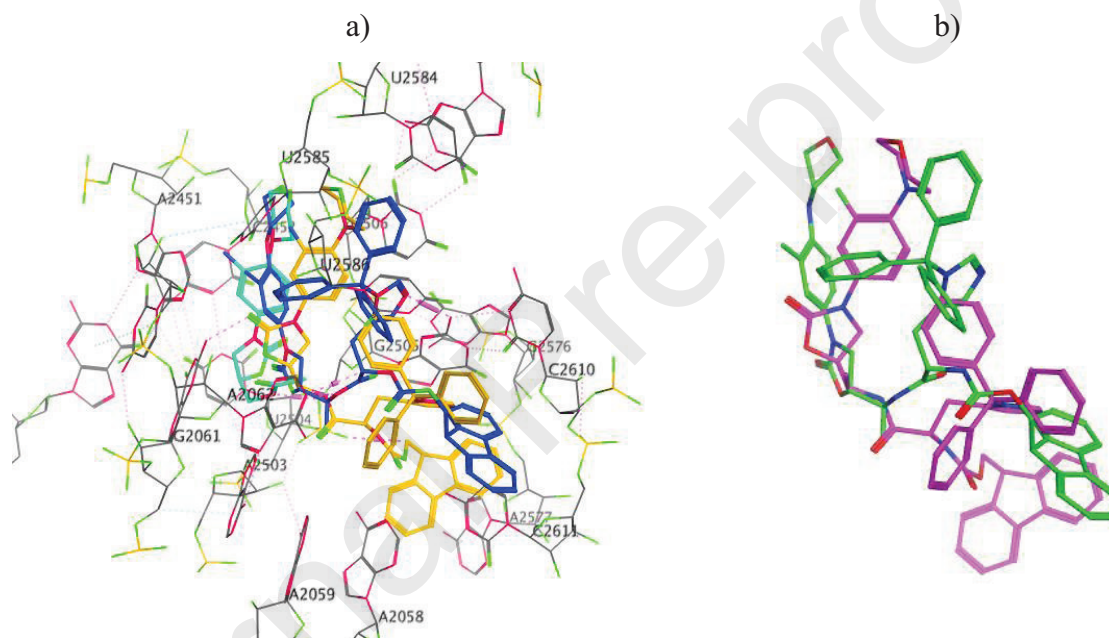


**Figure 8.** a) Molecular docking of Linezolid (magenta), **9ay** (blue) and **10ay** (yellow) and in PTC. b) Overlap structures of **9ay** (pink) and **10ay** (green).

### 3.4 Antibacterial activity against multidrug-resistant *Mycobacterium tuberculosis* clinical isolates.

First, all Linezolid dipeptide-type analogues were evaluated against three multidrug-resistant *Mycobacterium tuberculosis* clinical isolates by a BACTEC MGIT 960 method in a screening experiment at 125 mg/mL. The active analogues found in the experiment are L-Phenylalanine derivatives **9bs**, **9bw**, **9bt**, **9bu**, **10bs** and **10bw** (Figure 9), and two L-Alanine

derivatives (**9aw** and **10aw**). All analogues with Threonine as AA have shown significant activity (**9aw**, **10aw**, **9bw** and **10bw**). The *R,S,S* and *S,S,S* analogues with a benzyl as R<sub>1</sub> and R<sub>2</sub> (**9bs** and **10bs**) also display activity. These results suggest that inhibitory activity may be partially attribute to the presence of aromatic groups.

**Table 4.** Antibacterial activity evaluation of Linezolid analogues against multidrug-resistant *Mycobacterium tuberculosis* clinical isolates (MIC: µg/mL).

Compound	Diastereomer	R <sub>1</sub>	AA	Clinical isolate		
				820	1143	1083
<b>9aw</b>	<i>R,S,S</i>	CH <sub>3</sub>	Thr	-	-	125
<b>10aw</b>	<i>S,S,S</i>	CH <sub>3</sub>	Thr	-	-	125
<b>9bw</b>	<i>R,S,S</i>	Bn	Thr	100	100	R
<b>10bw</b>	<i>S,S,S</i>	Bn	Thr	R	100	100
<b>9bs</b>	<i>R,S,S</i>	Bn	Phe	125	125	R
<b>10bs</b>	<i>S,S,S</i>	Bn	Phe	R	125	R
<b>9bt</b>	<i>R,S,S</i>	Bn	Tyr	12.5	R	100
<b>9bu</b>	<i>R,S,S</i>	Bn	Leu	1.90	3.125	R
<b>Linezolid</b>	-	-	-	1.56	1.56	1.56

820: Resistant to isoniazid and rifampin

1143: Resistant to isoniazid, ethambutol and pyrazinamide

1083: Resistant to isoniazid, rifampin and streptomycin

A dilution experiment with the active analogues and Linezolid as control was performed. The most active analogues are **9bt** and **9bu** with MIC values of 12.5 µg/mL and 1.90 µg/mL, respectively (Table 4). Analogue **9bu** is the most active against two clinical isolates with a MIC values close to Linezolid. In addition, analogue **9bt** display a significant activity against one clinical isolate. The rest of the active analogues presented high MIC values (100 and 125 µg/mL), but interestingly, there are differences in the clinical isolate target depending on their stereochemistry.

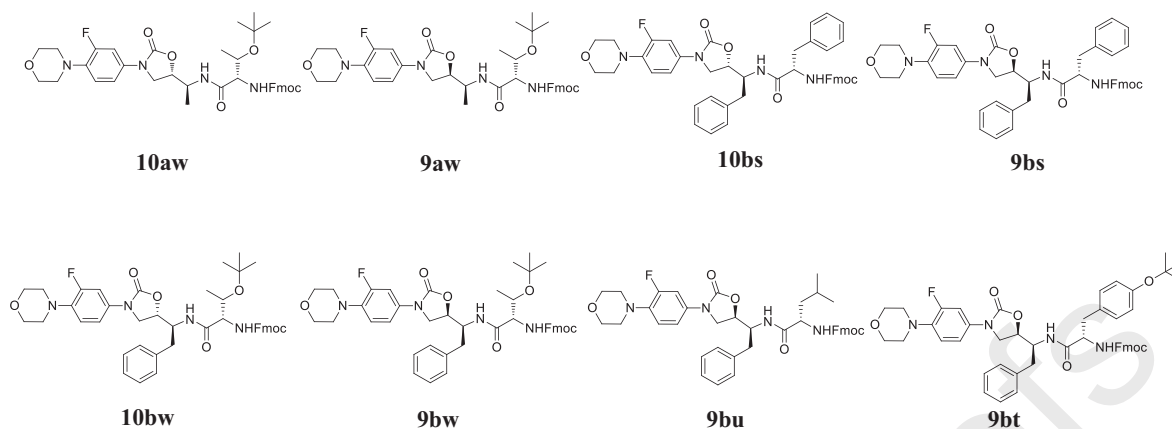


**Figure 9.** Active Linezolid dipeptide-type analogues against multidrug-resistant *Mycobacterium tuberculosis* clinical isolates.

As previously described, molecular docking of **9bu** shows a non-Linezolid like pose in PTC, establishing  $\pi$ - $\pi$ ,  $\sigma$ - $\pi$  and two hydrogen bond with G2505 (Figure 4), which is consistent with its significant antibacterial activity. Analogue **9bs** shows a similar pose than Linezolid and establish a hydrogen bond and  $\sigma$ - $\pi$  interaction with G2505 nucleotide, the Fmoc group is not involve in the interaction (Figure S99). The rest of active analogues display non-typical interactions with G2505 nucleotide and other nucleotides. For example, analogue **9bt** shows a  $\pi$ - $\pi$  interaction between a benzyloxy ring and A2062 nucleotide, and a hydrogen bond between the C ring-oxygen and G2583 nucleotide (Figure S100). Analogue **9bw** displays two  $\sigma$ - $\pi$  interactions between Fmoc group and Guanine base in G2505 nucleotide, the rest of molecule structure is not involved. The **10bw** analogue has a  $\sigma$ - $\pi$  interaction where a tertbutyl protecting group and Guanine base in G2505 nucleotide participate (Figures S101-S102).

Table S13 lists interaction type and distances observed in the molecular docking of Linezolid dipeptide-type analogues. As seen, the distance of donor-acceptor atoms are in the range of 2.8 y 4.6 Å. In addition, most of Linezolid analogues interact with G2505 acting as hydrogen bond donors, although there are some examples where act as acceptors or establish  $\sigma$ - $\pi$  or  $\pi$ - $\pi$  interactions. Some analogues display interaction with other nucleotides as G2061 (**10ay** and its non-protected analogue), A2451 (**9bu** and **9bt**), A2062 (**9as** and **9ay**) and G2583 (**9bt**). Molecular properties as LogP<sub>ow</sub>, H-donor and H-acceptor number, molecular weight (MW) and total polar surface area (TPSA) were calculated in order to

predict if these analogues might have good permeability and distribution if supplied orally (Lipinski's rule or the rule of 5).<sup>42,43</sup> LogP<sub>ow</sub> and TPSA values indicate these Linezolid dipeptide-type analogues display superior lipophilicity than Linezolid, as result of an increased of MW and the presence of protecting groups (Table S14).

### 3.5 Cellular viability

In order to evaluate whether Linezolid dipeptide-type analogues (**10as**, **10ay**, **9as**, **9ay**, **9aw**, **9ax** and **9bu**) induce a cytotoxic or inhibitory effect over the proliferation of ARPE-19 human cells, we carried out the cytocompatibility assays to evaluate their effect after 48 h of treatment (Table 5).<sup>47,48</sup> The Linezolid dipeptide-type analogues were tested until 100  $\mu\text{M}$  due to all the compounds were insoluble in the culture media at higher concentration (Figure S103). The results showed no significant reduction on cell viability or proliferation, remaining proliferation percentages over 80%. Interestingly, the **10ay** analogue preserves the viability until a 25  $\mu\text{M}$ , which is a seven-fold the MIC concentration (3.42  $\mu\text{M}$ ) obtained in the antibacterial assay. This compound present cytotoxicity at higher concentration (50 and 100 $\mu\text{M}$ ), reducing the cellular proliferation percentage and affecting the cellular morphology. In comparison, the cytotoxic positive control Doxorubicin, induced a strong cytotoxic antiproliferative effect over ARPE-19 cells, reducing cell proliferation by approximately 50% at a concentration of 0.125 $\mu\text{M}$ .

The exposure of the ARPE-19 cells to the Linezolid dipeptide-type analogues resulted in the maintenance of metabolic activity, viability and cellular integrity, indicating non-cytotoxic effects due to the Linezolid analogues treatments. Figures of micrographs depicting the cellular morphology of ARPE-19 cells treated with the Linezolid analogues, as well as controls are presented in supporting material (Figure S104).

**Table 5.** Proliferation percentages of ARPE-19 cells culture with Linezolid dipeptide-type analogues at 50  $\mu\text{M}$ .

<b>9as</b>	92.9 $\pm$ 4.5
<b>9ay</b>	86.3 $\pm$ 1.5
<b>9aw</b>	84.3 $\pm$ 4.6
<b>9ax</b>	88.8 $\pm$ 2.9

<b>9bu</b>	92.5 ± 10.7
<b>10as</b>	93.7 ± 7.5
<b>10ay</b>	71.9 ± 4.3 <sup>c</sup>
<b>Linezolid</b>	85.2 ± 4.7

<sup>a</sup> Data is expressed as mean of three independent experiments performed by triplicate.

<sup>b</sup> Doxorubicin was employed as a control.

<sup>c</sup> This result was obtained at 25 μM.

#### 4. Conclusions

Molecular docking of new Linezolid dipeptide-type analogues in PTC of *E. coli* used as model predicted different interactions as  $\sigma$ - $\pi$  and  $\pi$ - $\pi$  and different hydrogen bond interactions including the well-known interaction of the amide hydrogen with the G2505 and other nucleotides. The nature and number of the interactions with the active site as well as the cooperative effect of these interactions result in high thermodynamic stability and more favorable couplings, which may retard bacterial resistance towards these analogues. Most active analogues display better scoring than Linezolid in the molecular docking analysis. The results of antimicrobial activity point analogue **10ay** as the most active compound due to its comparable or even higher activity than Linezolid against three clinical isolates of MRSA. The tests against *Mycobacterium tuberculosis* strains showed **9bu** analogue as potential antituberculosis drug, due to its activity against multidrug-resistant clinical isolates with MICs close to Linezolid. The protecting groups increase the molecular weight in an acceptable range and their lipophilicity is highly superior to Linezolid, which may be beneficial to the cellular penetration. Noteworthy, the analogues **9bu** and **10ay** preserve the cellular integrity and metabolic viability of ARPE-19 indicating non-cytotoxic effects at concentration highly superior to their MIC values. We are currently conducting our efforts to the synthesis of non-protected Linezolid dipeptide-type analogues with increased solubility in aqueous culture media. Base on the molecular docking analysis these analogues with acceptor or donor hydrogen bond groups may increase the number of supramolecular interactions in PTC, and thereby, result in an improve biological activity.

## 5. – Experimental section

### 5.1 Chemistry

Reagents and solvents obtained from commercial suppliers were used without previous purification. The reactions with anhydrous conditions requirements were carry on Ar atmosphere. The nuclear magnetic resonance was carried out in a Bruker Advance III HD 400 MHz equipped with an intern reference of tetramethylsilane (TMS). The FTIR spectra were recorder on a Perkin Elmer Spectrum 400 FTIR spectrometer. The melting points were obtained in an Electrothermal apparatus. The electrospray ionization mass spectra (ESI/MS) were obtained on 6130 Quadrupole LC/MS of Agilent Technologies, in negative and positive ion modes.

### 5.2. Synthesis of compounds

***N*-aryl coupling.** To a mixture of the oxazolidinone (**2a-b** or **3a-b**) (0.32 mmol), CuI (0.01 mmol), K<sub>2</sub>CO<sub>3</sub> (0.53 mmol) and *N,N'*-dimethylmethanediamine (0.06 mmol) in 25 mL toluene was added 4-(4-bromo-2-fluorophenyl)morpholine (**1**) (0.32 mmol). The reaction mixture was stirred at 115°C for 72 h. Then, water (25 mL) was added to stop the reaction and the organic phase was separated, filtered in zeolite and the solvent was evaporated. The product purification was carried out by flash chromatography usign silica gel and a mixture of petroleum ether and ethyl acetate (1:1) as eluent.

**(*R*)-5-((*S*)-1-(dibenzylamino)ethyl)-3-(3-fluoro-4-morpholinophenyl)oxazolidin-2-one (**4a**).** White solid, yield 75 %. M.p. 68.5-69.5 °C FTIR: 3059, 2955, 1753, 1514, 1449, 1402, 1234, 1117 cm<sup>-1</sup>. <sup>1</sup>H NMR (400 MHz, CDCl<sub>3</sub>): δ 7.30 (m, 10 H), 7.18 (dd, *J*= 11.8, 2.5 Hz, 1H), 7.00 (ddd, *J*= 7.1, 2.5, 1.0 Hz, 1H), 6.89 (dd, *J*= 9.1, 9.0 Hz, 1H), 4.38 (ddd, *J*= 8.3, 8.2, 7.2 Hz, 1H), 3.86 (m, 4H), 3.80 (t, *J*= 8.7 Hz, 1H), 3.75(d, *J*= 13.5 Hz, 2H), 3.57 (dd, *J*= 9.0, 6.6 Hz, 1H), 3.48 (d, *J*= 13.5 Hz, 2H), 3.04 (m, 4H) 2.87 (dc, *J*= 8.9, 6.6 Hz, 1H), 1.28 (d, *J*= 6.6 Hz, 3H). <sup>13</sup>C NMR (100 MHz, CDCl<sub>3</sub>): δ 155.5 (d, *J*<sub>C-F</sub>= 244.4 Hz), 154.6, 139.1, 136.2 (d, *J*<sub>C-F</sub>= 9.0 Hz) 133.3 (d, *J*<sub>C-F</sub>= 10.5 Hz), 128.9, 128.5, 127.4, 118.7 (d, *J*<sub>C-F</sub>= 4.1 Hz), 114.2 (d, *J*<sub>C-F</sub>= 3.3 Hz), 107.7 (d, *J*<sub>C-F</sub>= 25.8 Hz), 74.2, 66.9, 56.7, 54.6, 51.9, 49.4, 8.6. MS(IE) *m/e* 489(5), 224(100), 91(90).

**(R)-5-((S)-1-(dibenzylamino)-2-phenylethyl)-3-(3-fluoro-4-**

**morpholinophenyl)oxazolidin-2-one (4b).** White solid, yield 60%. FTIR: 3029, 2826, 1748, 1513, 1110  $\text{cm}^{-1}$ .  $^1\text{H}$  NMR (400 MHz,  $\text{CDCl}_3$ ):  $\delta$  7.38 (dd,  $J_1=13.5$ ,  $J_2=2.6$  Hz, 1H), 7.13 (m, 15H), 7.13 (m, 3H), 7.04 (t,  $J=9.2$  Hz, 1H), 4.99 (m, 1H), 4.06 (t,  $J=9.0$  Hz, 1H), 3.74 (m, 4H), 3.64 (m, 6H), 3.00 (dc, 1H), 2.96 (m, 1H).  $^{13}\text{C}$  NMR (100 MHz,  $\text{CDCl}_3$ ):  $\delta$  155.0 ( $J=245.8$  Hz), 154.5, 140.3, 139.7, 127.4, 126.5, 119.7, 114.7, 107.2 ( $J=25.7$ ), 72.9, 66.6, 62.7, 54.2, 51.2 ( $J=2.5$  Hz), 49.0, 31.9. MS(IE)  $m/e$  565(5), 474(30), 383(10), 91(80).

**((S)-5-((S)-1-(dibenzylamino)ethyl)-3-(3-fluoro-4-morpholinophenyl)oxazolidin-2-one**

**(5a).** White solid, yield 70 %. M.p. 78.0-79.0  $^\circ\text{C}$ . FTIR: 3032, 2955, 1753, 1514, 1449, 1402, 1234, 1117  $\text{cm}^{-1}$ .  $^1\text{H}$  NMR (400 MHz,  $\text{CDCl}_3$ ):  $\delta$  7.37 (dd,  $J=11.8$ , 2.6 Hz, 1H), 7.30 (m, 10 H), 7.00 (ddd,  $J=7.3$ , 2.0, 1.3 Hz, 1H), 6.94 (dd,  $J=9.2$ , 9.0 Hz, 1H), 4.56 (ddd,  $J=5.4$ , 5.1, 5.1 Hz, 1H), 3.93 (d,  $J=13.6$  Hz, 2H), 3.88 (m, 4H), 3.68 (dd,  $J=8.4$ , 2.4 Hz, 1H), 3.48 (d,  $J=13.6$  Hz, 2H), 3.07 (m, 4H), 2.92 (dc,  $J=6.8$ , 5.1 Hz, 1H), 1.26 (d,  $J=6.8$  Hz, 3H).  $^{13}\text{C}$  NMR (100 MHz  $\text{CDCl}_3$ ):  $\delta$  155.5 (d,  $J_{\text{C-F}}=244.5$  Hz), 154.5, 139.6, 136.2 (d,  $J_{\text{C-F}}=8.9$  Hz), 133.5 (d,  $J_{\text{C-F}}=10.5$  Hz), 128.9, 128.3, 127.0, 118.7 (d,  $J_{\text{C-F}}=4.2$  Hz), 113.7 (d,  $J_{\text{C-F}}=3.3$  Hz), 107.3 (d,  $J_{\text{C-F}}=26.3$ ), 76.2, 67.0, 55.1, 54.8, 51.0, 47.6, 10.2. MS(IE)  $m/e$  489(5), 224(100), 91(90).

**(S)-5-((S)-1-(dibenzylamino)-2-phenylethyl)-3-(3-fluoro-4-**

**morpholinophenyl)oxazolidin-2-one (5b).** White solid, yield 60%. FTIR: 3029, 2826, 1748, 1513, 1110  $\text{cm}^{-1}$ .  $^1\text{H}$  NMR (400 MHz,  $\text{CDCl}_3$ ):  $\delta$  7.36 (m, 1H), 7.34-7.20 (m, 15H), 7.07 (d,d,  $J_1=9.5$  Hz,  $J_2=2.5$  Hz, 1H), 6.95 (t,  $J=9.2$  Hz, 1H), 4.48 (m, 1H), 4.08 (d, 2H), 3.89 (m, 4H), 3.73 (d,d,  $J_1=8.0$  Hz,  $J_2=6.6$  Hz, 1H), 3.55 (d, 2H), 3.47 (d,d,  $J_1=9.1$  Hz,  $J_2=8.3$  Hz, 1H), 3.23 (m, 2H), 3.09 (m, 4H), 2.81 (d,t,  $J_1=10.6$  Hz,  $J_2=3.6$  Hz, 1H).  $^{13}\text{C}$  NMR (100 MHz,  $\text{CDCl}_3$ ):  $\delta$  154.5, 139.3, 138.8, 136.1 (d,  $J=9.0$  Hz), 133.5 (d,  $J=10.3$  Hz), 129.5, 129.1, 128.8, 128.4, 127.2, 126.5, 118.8 (d,  $J=3.6$  Hz), 113.7 (d,  $J=3.1$  Hz), 107.2 (d,  $J=26.0$  Hz), 72.9, 67.0, 61.2, 55.9, 51.1 (d,  $J=3.6$  Hz), 46.8, 30.9.

**Hydrogenolysis.** The compounds **4a-b** or **5a-b** (0.06 mmol) were dissolved in dry methanol (50 mL) and Pd/C 10% (4.1 mmol) was added. Then, three acetic acid drops were added and the reaction mixture was stirred for 4 h under  $\text{H}_2$  atmosphere. Then, the Pd/C was filtered and the organic solvent was evaporated to obtain an analytical pure product.

**(R)-5-((S)-1-aminoethyl)-3-(3-fluoro-4-morpholinophenyl)oxazolidin-2-one (6a).** White solid, yield 90 %. M.p. 196-197 °C. FTIR: 3373, 2952, 2835, 1740, 1636, 1514, 1445, 1404, 1237, 1112  $\text{cm}^{-1}$ .  $^1\text{H}$  NMR(400 MHz,  $\text{CDCl}_3$ ):  $\delta$  7.45 (dd,  $J=$  11.8, 2.6 Hz, 1H), 7.15 (ddd,  $J=$  8.8, 1.5, 1.2 Hz, 1H), 6.92 (dd,  $J=$  9.1, 9.0 Hz, 1H), 4.48 (ddd,  $J=$  8.4, 8.1, 7.2 Hz, 1H), 3.92 (dd,  $J=$  8.5, 1.6 Hz, 2H), 3.87(m, 4H), 3.34 (m, 1H), 3.05 (m, 4H) 1.19 (d,  $J=$  6.6 Hz, 3H).  $^{13}\text{C}$  NMR(100 MHz,  $\text{CDCl}_3$ ):  $\delta$  155.5 (d,  $J_{\text{C-F}}=$  220.4 Hz), 154.6, 136.2 (d,  $J_{\text{C-F}}=$  7.3 Hz) 133.4 (d,  $J_{\text{C-F}}=$  10.2 Hz), 118.8 (d,  $J_{\text{C-F}}=$  4.1 Hz), 113.8 (d,  $J_{\text{C-F}}=$  3.3 Hz), 107.4 (d, 26.1), 76.2, 67.0, 51.1, 48.2, 46.2, 17.7. MS(IE)  $m/e$  309(100), 209(90), 164(50), 44(90).

**(R)-5-((S)-1-amino-2-phenylethyl)-3-(3-fluoro-4-morpholinophenyl)oxazolidin-2-one (6b).** White solid, yield 95 %. FT-IR 3052, 2925, 1753, 1515, 1234  $\text{cm}^{-1}$ .  $^1\text{H}$  NMR (400 MHz,  $\text{CDCl}_3$ ):  $\delta$  7.55 (d,  $J_{\text{I}}=$ 15.1 Hz, 1H), 7.28 (m, 6H), 7.07 (t, 9.4 Hz, 1H), 4.48 (m, 1H), 3.98 (m, 2H), 3.74 (m, 4H), 3.18 (m, 1H), 2.97 (m, 4H), 2.76 (m, 2H).  $^{13}\text{C}$  NMR (100 MHz,  $\text{CDCl}_3$ ):  $\delta$  154.6 ( $J=$  241.1 Hz, C-F), 154.7, 138.9, 135.8, 134.2, 134.1, 129.8, 126.6, 119.7, 114.5, 107.2 ( $J=$ 25.7, CH), 75.8, 66.6, 54.7, 51.2, 46.3, 35.3.

**(S)-5-((S)-1-aminoethyl)-3-(3-fluoro-4-morpholinophenyl)oxazolidin-2-one (7a).** White solid, yield 80 %. M.p. 128-129 °C. FTIR: 3373, 2956, 1744, 1625, 1514, 1407, 1234, 1114  $\text{cm}^{-1}$ .  $^1\text{H}$  NMR (400 MHz,  $\text{CDCl}_3$ ):  $\delta$  7.51 (dd,  $J=$  12.4, 2.6 Hz, 1H), 7.23 (dd,  $J=$  8.8, 1.9 Hz, 1H), 7.05 (dd,  $J=$  9.8, 9.1 Hz, 1H), 4.45 (ddd,  $J=$  8.7, 8.6, 7.8 Hz, 1H), 4.01 (dd,  $J=$  9.0, 8.9 Hz, 1H), 3.83 (dd,  $J=$  9.0, 8.9 Hz, 1H), 3.73 (m, 4H), 3.02 (m, 1H), 2.96 (m, 4H), 1.05 (d,  $J=$  6.5 Hz, 3H).  $^{13}\text{C}$  NMR (100 MHz,  $\text{CDCl}_3$ ):  $\delta$  155.5 (d,  $J_{\text{C-F}}=$  242.1 Hz), 154.7, 135.8 (d,  $J_{\text{C-F}}=$  8.8 Hz) 134.1 (d,  $J_{\text{C-F}}=$  10.4 Hz), 119.7 (d,  $J_{\text{C-F}}=$  4.2 Hz), 114.4 (d,  $J_{\text{C-F}}=$  3.2 Hz), 107.3 (d,  $J_{\text{C-F}}=$  26.0 Hz), 75.8, 66.6, 51.2, 49.2, 47.1, 18.2. MS(IE)  $m/e$  309(100), 209(90), 164(50), 44(90).

**(S)-5-((S)-1-amino-2-phenylethyl)-3-(3-fluoro-4-morpholinophenyl)oxazolidin-2-one (7b).** White solid, yield 95%. FT-IR 3050, 2923, 1751, 1513, 1232  $\text{cm}^{-1}$ .  $^1\text{H}$  NMR (400 MHz,  $\text{CDCl}_3$ ):  $\delta$  7.55 (d,  $J_{\text{I}}=$ 15.1 Hz, 1H), 7.28 (m, 6H), 7.07 (t, 9.4 Hz, 1H), 4.48 (m, 1H), 3.98 (m, 2H), 3.74 (m, 4H), 3.18 (m, 1H), 2.97 (m, 4H), 2.76 (m, 2H).  $^{13}\text{C}$  NMR (100 MHz,  $\text{CDCl}_3$ ):  $\delta$  154.6 ( $J=$  241.1 Hz), 154.7, 138.9, 135.8, 134.2, 134.1, 129.8, 126.6, 119.7, 114.5, 107.2 ( $J=$ 25.7), 75.8, 66.6, 54.7, 51.2, 46.3, 35.3.

**Peptide coupling with protected L-amino acids.** *N*-Fmoc  $\alpha$ -amino acids (**8s-z**) (0.13 mmol) were dissolved in DMF (10 mL) and then DIC (0.15 mmol) and HOBt (0.15 mmol) were added. The mixture was stirred for 20 min and then the compound (**6a-b** or **7a-b**) (0.13 mmol) was added. The reaction mixture was stirred for 12 h. Distilled water was added to stop the reaction and a solid product was filtered and repeatedly washed with water. The compounds were dried under vacuum at RT.

**(9H-fluoren-9-yl)methyl ((S)-1-(((S)-1-((R)-3-(3-fluoro-4-morpholinophenyl)-2-oxooxazolidin-5-yl)ethyl)amino)-1-oxo-3-phenylpropan-2-yl)carbamate (9as).** White solid, yield 55 %. M.p. 135.5-136.5 °C FTIR: 3293 3023, 2955, 1754, 1699, 1656, 1514, 1448, 1226, 1106  $\text{cm}^{-1}$ .  $^1\text{H}$  NMR (400 MHz,  $\text{CDCl}_3$ ):  $\delta$  7.75 (d,  $J=7.5$  Hz, 2H), 7.52 (t,  $J=6.5$  Hz, 2H), 7.37 (m, 3H), 7.28 (m, 5 H), 7.18 (m, 2H), 7.06 (m, 1H), 6.89 (t,  $J=9.1$ , 1H), 6.35 (sa, 1H), 5.40 (sa, 1H), 4.43 (m, 3H), 4.29 (m, 1H), 4.17 (t,  $J=6.7$  Hz, 1H), 4.13 (m, 1H), 3.85 (m, 4H), 3.75 (t,  $J=9.1$  Hz, 1H), 3.56 (m, 1H), 3.04 (m, 6H), 1.15 (d,  $J=6.3$  Hz, 3H).  $^{13}\text{C}$  NMR (100 MHz,  $\text{CDCl}_3$ ):  $\delta$  170.1, 156.0, 155.9, 155.5 (d,  $J_{\text{C-F}}=246.1$  Hz), 154.6, 143.6, 141.3, 136.7 (d,  $J_{\text{C-F}}=8.6$  Hz), 136.1, 132.8 (d,  $J_{\text{C-F}}=10.1$  Hz), 129.2, 128.7, 127.7, 127.2, 127.0, 125.0, 120.0, 118.8 (d,  $J_{\text{C-F}}=4.1$  Hz), 114.0 (d,  $J_{\text{C-F}}=3.2$  Hz), 107.5 (d, 26.1), 74.3, 67.1, 66.9, 56.3, 51.0, 47.8, 47.7, 47.1, 38.0, 14.4. MS(ESI): 679  $[\text{M}+\text{H}]^+$ , 701  $[\text{M}+\text{Na}]^+$ , 717  $[\text{M}+\text{K}]^+$ .

**(9H-fluoren-9-yl)methyl ((S)-3-(4-(tert-butoxy)phenyl)-1-(((S)-1-((R)-3-(3-fluoro-4-morpholinophenyl)-2-oxooxazolidin-5-yl)ethyl)amino)-1-oxopropan-2-yl)carbamate (9at).** White solid, yield 38 %. M.p. 115.5-116.5 °C FTIR: 3294, 3023, 2976, 1748, 1710, 1655, 1513, 1448, 1227, 1105  $\text{cm}^{-1}$ .  $^1\text{H}$  NMR (400 MHz,  $\text{CDCl}_3$ ):  $\delta$  7.72 (d,  $J=7.5$  Hz, 2H), 7.53 (dd,  $J=7.2, 6.9$  Hz, 2H), 7.40 (dd,  $J=12.1, 2.1$  Hz, 1H), 7.36 (m, 2 H), 7.26 (m, 2H), 7.08 (d,  $J=6.8, 2\text{H}$ ), 7.01 (d,  $J=8.3$  Hz, 1H), 6.89 (d,  $J=7.6$  Hz, 3H), 5.87 (sa, 1H), 4.48 (m, 1H), 4.32 (m, 3H), 4.13 (m, 2H), 3.83 (m, 4H), 3.76 (t,  $J=8.7$  Hz, 1H), 3.57 (t,  $J=6.4$  Hz, 1H), 3.00 (m, 6H), 1.26 (sa, 9H), 1.13 (d,  $J=5.8$  Hz, 3H).  $^{13}\text{C}$  NMR (100 MHz,  $\text{CDCl}_3$ ):  $\delta$  171.0, 156.0, 155.5 (d,  $J_{\text{C-F}}=245.1$  Hz), 154.5, 154.4 143.6, 141.2, 136.4 (d,  $J_{\text{C-F}}=8.9$  Hz), 133.0 (d,  $J_{\text{C-F}}=10.4$  Hz), 131.0, 129.2, 128.7, 127.8, 127.5, 127.0, 124.9, 124.2 119.9, 118.8 (d,  $J_{\text{C-F}}=4.1$  Hz), 114.0 (d,  $J_{\text{C-F}}=3.2$  Hz), 107.5 (d,  $J_{\text{C-F}}=26.1$ ), 78.4, 74.3, 67.1, 66.9, 56.3, 51.0, 47.8, 47.7, 47.1, 38.4, 28.7, 14.4. MS(ESI): 751  $[\text{M}+\text{H}]^+$ , 773  $[\text{M}+\text{Na}]^+$ , 789  $[\text{M}+\text{K}]^+$ .

**(9H-fluoren-9-yl)methyl ((S)-1-(((S)-1-((R)-3-(3-fluoro-4-morpholinophenyl)-2-oxooxazolidin-5-yl)ethyl)amino)-4-methyl-1-oxopentan-2-yl)carbamate (9au).** White solid, yield 38 %. M.p. 102.0-103.0 °C. FTIR: 3295, 3023, 2956, 1749, 1716, 1656, 1514, 1448, 1226, 1106 cm<sup>-1</sup>. <sup>1</sup>H NMR (400 MHz, CDCl<sub>3</sub>): δ 7.78 (d, *J*= 7.4 Hz, 2H), 7.71 (m, 1H), 7.58 (d, *J*= 7.2 Hz, 2H), 7.41 (t, *J*= 7.5 Hz, 2H), 7.37 (m, 1H), 7.32 (t, *J*= 7.5 Hz, 2H), 7.06 (m, 1H), 6.41 (sa, 1H), 5.21 (sa, 1H), 4.60 (m, 1H), 4.37 (m, 2H), 4.13 (m, 3H), 4.12 (m, 4H), 4.00 (m, 1H), 3.78 (m, 1H), 3.38 (m, 4H), 1.65 (m, 1H), 1.54 (m, 2H), 1.25 (d, *J*= 5.9 Hz, 3H), 0.95 (sa, 6H). <sup>13</sup>C NMR (100 MHz, CDCl<sub>3</sub>): δ 172.3, 155.5 (d, *J*<sub>C-F</sub>= 254.2 Hz), 155.0, 154.5, 143.6, 141.2, 136.4 (d, *J*<sub>C-F</sub>= 7.0 Hz), 133.0 (d, *J*<sub>C-F</sub>= 10.0 Hz), 127.8, 127.0, 124.8, 120.0, 118.8 (d, *J*<sub>C-F</sub>= 5.4 Hz), 114.0 (d, *J*<sub>C-F</sub>= 4.0 Hz), 107.8 (d, *J*<sub>C-F</sub>= 25.1 Hz), 74.7, 67.0, 65.4, 53.6, 52.3, 47.7, 47.5, 47.1, 41.1, 24.7, 22.9, 14.3. MS(ESI): 645 [M+H]<sup>+</sup>, 667 [M+Na]<sup>+</sup>, 683 [M+K]<sup>+</sup>.

**(9H-fluoren-9-yl)methyl ((2S)-3-(tert-butoxy)-1-(((S)-1-((R)-3-(3-fluoro-4-morpholinophenyl)-2-oxooxazolidin-5-yl)ethyl)amino)-1-oxobutan-2-yl)carbamate (9aw).** White solid, yield 35 %. M.p. 84.5-86.5.0 °C FTIR: 3300, 3023, 2973, 1749, 1719, 1670, 1514, 1448, 1224, 1048 cm<sup>-1</sup>. <sup>1</sup>H NMR (400 MHz, CDCl<sub>3</sub>): δ 7.77 (dd, *J*= 7.4, 5.4 Hz, 2H), 7.61 (d, *J*= 7.5 Hz, 3H), 7.42 (dd, *J*= 7.3, 7.0 Hz, 3H), 7.33 (dd, *J*= 7.5, 7.0 Hz, 2H), 7.10 (m, 1H), 5.09 (sa, 1H), 4.64 (m, 1H), 4.41 (m, 2H), 4.25 (m, 2H), 4.18 (m, 2H), 4.01 (m, 5H), 3.86 (m, 1H), 3.24 (m, 4H), 1.29 (s, 9H), 1.24 (s, 3H), 1.08 (d, *J*= 6.3 Hz, 3H). <sup>13</sup>C NMR (100 MHz, CDCl<sub>3</sub>): δ 169.7, 156.0, 155.9, 155.4 (d, *J*<sub>C-F</sub>= 258.1 Hz), 143.6, 141.3, 127.8, 127.0, 125.0, 120.0, 119.9 (d, *J*<sub>C-F</sub>= 7.4 Hz), 113.8 (d, *J*<sub>C-F</sub>= 3.4 Hz), 107.7 (d, 26.4), 75.7, 74.5, 66.9, 66.5, 66.1, 58.9, 51.7, 47.8, 47.7, 47.2, 28.2, 17.2, 14.7. MS(ESI): 689 [M+H]<sup>+</sup>, 711 [M+Na]<sup>+</sup>, 729 [M+K]<sup>+</sup>.

**(9H-fluoren-9-yl)methyl ((R)-3-(tert-butylthio)-1-(((S)-1-((R)-3-(3-fluoro-4-morpholinophenyl)-2-oxooxazolidin-5-yl)ethyl)amino)-1-oxopropan-2-yl)carbamate (9ax).** White solid, yield 36 %. M.p. 91.5-92.5 °C. FTIR: 3296, 3008, 2951, 1754, 1714, 1675, 1514, 1232, 1110 cm<sup>-1</sup>. <sup>1</sup>H NMR (CDCl<sub>3</sub>, 400 MHz): δ 7.74 (m, 2H), 7.55 (m, 2H), 7.39 (m, 9H), 7.26 (m, 8H), 7.20 (m, 3H), 7.01 (d, *J*= 9.2 Hz, 1H), 6.83 (t, *J*= 9.1 Hz, 1H), 6.00 (d, *J*= 8.6 Hz, 1H), 5.00 (d, *J*= 7.3 Hz, 1H), 4.41 (m, 1H), 4.20 (m, 3H), 4.12 (m, 1H), 3.91 (t, *J*= 9.1 Hz, 1H), 3.80 (m, 4H), 3.75 (dd, *J*= 7.0, 6.9 Hz, 1H), 3.69 (dd, *J*= 9.0, 6.6 Hz, 1H),

3.02 (m, 4H), 2.62 (d,  $J=6.5$  Hz, 2H), 1.18 (d,  $J=6.7$  Hz, 3H).  $^{13}\text{C}$  NMR ( $\text{CDCl}_3$ , 100 MHz):  $\delta$  170.0, 160.0 (d,  $J=233.2$  Hz), 155.9, 155.7, 144.0, 143.5, 141.3, 136.0 (d,  $J=13.0$  Hz), 133.6 (d,  $J=12.1$  Hz), 129.4, 128.1, 127.8, 127.1, 127.0, 124.9, 120.0, 118.3 (d,  $J=6.1$  Hz), 113.0 (d,  $J=3.1$  Hz), 107.7 (d,  $J=29.3$  Hz), 79.2, 74.5, 68.1, 66.9, 54.8, 51.0, 47.9, 47.7, 47.0, 30.4, 14.0.

**(9H-fluoren-9-yl)methyl ((S)-1-(((S)-1-((R)-3-(3-fluoro-4-morpholinophenyl)-2-oxooxazolidin-5-yl)ethyl)amino)-1-oxo-3-(1-trityl-1H-imidazol-4-yl)propan-2-yl)carbamate (9ay)**. White solid, yield 36 %. M.p. 108.5-109.5 °C. FTIR: 3304, 3059, 2955, 1750, 1718, 1671, 1513, 1228, 1114  $\text{cm}^{-1}$ .  $^1\text{H}$  NMR ( $\text{CDCl}_3$ , 400 MHz):  $\delta$  7.70 (m, 3H), 7.50 (m, 3H), 7.36 (m, 3H), 7.30 (m, 6H), 7.24 (m, 2H), 7.21 (m, 9H), 6.94 (m, 1H), 6.70 (m, 1H), 6.43 (sa, 1H), 5.07 (sa, 1H), 4.50 (m, 1H), 4.31 (m, 1H), 4.21 (m, 2H), 4.09 (m, 1H), 3.80 (m, 5H), 3.75 (m, 2H), 2.93 (m, 4H), 2.57 (m, 2H), 1.27 (d,  $J=5.6$  Hz, 3H).  $^{13}\text{C}$  NMR ( $\text{CDCl}_3$ , 100 MHz):  $\delta$  170.6, 155.7, 155.5 (d,  $J=244.2$  Hz), 154.1, 143.6, 141.2, 138.7, 136.2 (d,  $J=8.8$  Hz), 133.1 (d,  $J=9.6$  Hz), 132.4, 130.9, 129.4, 128.7, 128.1, 127.7, 127.0, 126.9, 125.0, 119.9, 118.7 (d,  $J=4.3$  Hz), 113.9 (d,  $J=2.0$  Hz), 107.5 (d,  $J=27.5$  Hz), 85.9, 74.8, 67.4, 66.9, 54.3, 50.9, 47.4, 47.0, 45.7, 33.6, 17.7. MS(ESI):  $[\text{M}+\text{H}]^+=912$  amu,  $[\text{M}+\text{Na}]^+=934$  amu,  $[\text{M}+\text{K}]^+=950$  amu.

**(9H-fluoren-9-yl)methyl ((S)-3-(tert-butoxy)-1-(((S)-1-((R)-3-(3-fluoro-4-morpholinophenyl)-2-oxooxazolidin-5-yl)ethyl)amino)-1-oxopropan-2-yl)carbamate (9az)**. White solid, yield 36 %. M.p. 80.0-81.0 °C. FTIR: 3296, 3020, 2969, 1736, 1715, 1669, 1514, 1225, 1114  $\text{cm}^{-1}$ .  $^1\text{H}$  NMR ( $\text{CDCl}_3$ , 400 MHz):  $\delta$  7.73 (d,  $J=7.5$  Hz, 2H), 7.52 (d,  $J=9.4$  Hz, 2H), 7.38 (m, 2H), 7.30 (m, 3H), 7.00 (m, 1H), 6.84 (m, 1H), 4.65 (m, 1H), 4.22 (m, 3H), 4.15 (m, 2H), 3.82 (m, 6H), 3.75 (dd,  $J=9.2, 8.9$  Hz, 1H), 3.37 (dd,  $J=8.9, 8.6$  Hz, 1H), 2.97 (m, 4H), 1.37 (d,  $J=6.9$  Hz, 3H).  $^{13}\text{C}$  NMR ( $\text{CDCl}_3$ , 100 MHz):  $\delta$  171.0, 156.5 (d,  $J=225.2$  Hz), 156.1, 154.6, 143.9, 141.2, 137.0 (d,  $J=7.3$  Hz), 133.5 (d,  $J=7.1$  Hz), 127.6, 127.0, 125.0, 119.9, 118.8 (d,  $J=4.5$  Hz), 114.1 (d,  $J=4.0$  Hz), 107.6 (d,  $J=20.0$  Hz), 78.2, 75.2, 68.1, 66.8, 61.5, 56.1, 50.9, 47.7, 47.1, 46.3, 27.3, 17.9. MS(ESI):  $[\text{M}+\text{H}]^+=675$  amu,  $[\text{M}+\text{Na}]^+=697$  amu,  $[\text{M}+\text{K}]^+=713$  amu.

**(9H-fluoren-9-yl)methyl ((S)-1-(((S)-1-((R)-3-(3-fluoro-4-morpholinophenyl)-2-oxooxazolidin-5-yl)-2-phenylethyl)amino)-1-oxo-3-phenylpropan-2-yl)carbamate**

**(9bs).** White solid, yield 48%. M.p. 87-88 °C. FTIR: 3309, 3035, 2960, 1775, 1760, 1684, 1517, 1448, 1221 cm<sup>-1</sup>. <sup>1</sup>H NMR (400 MHz, CDCl<sub>3</sub>): δ 7.74(d, *J*= 7.6 Hz, 2H), 7.51 (d, *J*=9.6 Hz, 2H), 7.40-7.13 8m, 14H), 7.39 (d, *J*=7.9 Hz, 2H), 7.35 (m, 1H), 7.29 (m, 1H), 7.05 (d, *J*= 7.6 Hz, 1H), 6.91(t, *J*= 9.2 Hz, 1H), 4.61 (m, 1H), 4.39 (m, 1H), 4.32 (m, 1H), 4.24 (m, 2H), 4.20 (m,1H), 3.94(dd, *J*= 8.7, *J*=8.6 Hz, 1H), 3.86 (m, 4H), 3.66(dd, *J*= 8.3, *J*=8.2 Hz, 1H), 3.05 (m, 4H), 3.12 (m, 1H), 3.00 (m, 1H), 2.94 (m, 1H), 2.88 (m, 1H). <sup>13</sup>C NMR (100 MHz, CDCl<sub>3</sub>): δ 170.9, 155.0 (d, *J*<sub>C-F</sub>= 233 Hz), 154.9, 154.1, 143.7 (2 x C), 141.3 (2 x C), 136.9, 136.1, 136.0, 132.1, 130.9, 129.3 (2 x CH), 129.4 (2 x CH), 129.2 (2 x CH), 128.9 (2 x CH), 128.7, 127.8 (2 x CH), 127.1 (2 x CH), 125.1 (2 x CH), 120.0 (2 x CH), 118.8 (d, *J*<sub>C-F</sub>=3.8 Hz), 113.9 (d, *J*<sub>C-F</sub>= 3.2 Hz), 107.4 (d, *J*<sub>C-F</sub>=26.3 Hz), 73.1, 68.2, 66.9 (2 x CH<sub>2</sub>), 52.5, 52.2, 51.1 (2 x CH<sub>2</sub>), 48.8, 48.0, 38.8, 37.0. MS(ESI): 756 [M+2H]<sup>+</sup>.

**(9H-fluoren-9-yl)methyl ((S)-3-(4-(tert-butoxy)phenyl)-1-(((S)-1-((R)-3-(3-fluoro-4-morpholinophenyl)-2-oxooxazolidin-5-yl)-2-phenylethyl)amino)-1-oxopropan-2-**

**yl)carbamate (9bt).** White solid, yield 43%. M.p. 77-79 °C. FTIR: 3310, 3067, 2978, 1752, 1717, 1670, 1515, 1224, 1046 cm<sup>-1</sup>. <sup>1</sup>H NMR (400 MHz, CDCl<sub>3</sub>): δ 7.83 (d, *J*=7.5 Hz, 2H), 7.68 (t, *J*= 7.6Hz, 2H), 7.53 (m, 2H), 7.31 (m, 2H), 7.18 (m, 5H), 6.92 (m, 1H), 4.48 (m, 1H), 4.30 (m, 1H), 4.29 (m, 1H), 4.14 (m, 1H), 3.77 (m, 1H), 3.73 (m, 1H), 3.54 (m, 1H), 3.15 (m, 1H), 1.15 (sa, 1H). <sup>13</sup>C NMR (100 MHz, CDCl<sub>3</sub>): δ 176.7, 156.6, 155.6(d, *J*<sub>C-F</sub>=244.0), 154.7, 154.3, 143.8, 141.2, 139.0, 136.5, 135.4(d, *J*<sub>C-F</sub>=9.0), 132.5(d, *J*<sub>C-F</sub>=10.3), 129.4, 129.2, 128.8, 127.6, 127.1, 127.0, 125.0, 124.3, 119.9, 118.7(d, *J*<sub>C-F</sub>=2.9), 114.1(d, *J*<sub>C-F</sub>=3.7), 107.7(d, *J*<sub>C-F</sub>=26.0), 78.4, 72.4, 67.3, 64.5, 56.6, 53.1, 51.4, 47.3, 46.9, 38.0, 37.1, 28.8. MS(ESI): 826 [M+H]<sup>+</sup>.

**(9H-fluoren-9-yl)methyl ((S)-1-(((S)-1-((R)-3-(3-fluoro-4-morpholinophenyl)-2-oxooxazolidin-5-yl)-2-phenylethyl)amino)-4-methyl-1-oxopentan-2-yl)carbamate**

**(9bu).** White solid, yield 49%. M.p. 120-122 °C. FTIR: 3305, 3064, 2959, 1757, 1715, 1686, 1516, 1225, 1031 cm<sup>-1</sup>. <sup>1</sup>H NMR (400 MHz, CDCl<sub>3</sub>): δ 7.76 (d, *J*=7 Hz, 2H), 7.42 (m, 1H), 7.40 (m, 2H), 7.33 (m, 2H), 7.32 (m, 2H), 7.22-7.13 (m, 5H), 7.01 (d, *J*=7.1 Hz, 1H), 6.85 (t, *J*=9.1Hz, 1H), 4.56 (m,1H), 4.50 (m, 2H), 4.43 (m, 1H), 4.21 (m, 1H), 4.04 (m, 1H), 3.90 (m, 1H), 3.88 (m, 4H), 3.81 (m, 1H), 3.10 (dd, *J*=14.3, 4.4 Hz, 1H), 3.05 (m, 4H), 2.90 (dd, *J*=14.0, 9.8, 1H), 1.54 (m, 2H), 1.34 (m, 1H), 0.91-0.79 (m, 6H). <sup>13</sup>C NMR (100 MHz,

CDCl<sub>3</sub>):  $\delta$  172.4, 155.5 (d,  $J_{C-F}$  = 246 Hz), 154.3 (C=O), 154.2, 143.7, 141.4, 136.6, 136.0, 132.7, 129.2 (2 x CH), 128.7(2 x CH), 127.9, 127.7, 127.0, 124.9, 120.1, 118.8 (d,  $J_{C-F}$  = 4 Hz), 114.1 (d,  $J_{C-F}$  = 3 Hz), 107.7 (d,  $J_{C-F}$  = 26 Hz), 73.4, 67.0, 66.9 (2 x CH<sub>2</sub>), 53.4, 52.8, 51.0 (d,  $J_{C-F}$  = 3 Hz, 2 x CH<sub>2</sub>), 48.0, 47.2, 40.5, 38.8, 24.7, 22.8, 21.8. MS(ESI): 739 [M+H<sub>2</sub>O]<sup>+</sup>.

**(9H-fluoren-9-yl)methyl ((2S)-3-(3a,7a-dihydro-1H-indol-3-yl)-1-(((S)-1-((R)-3-(3-fluoro-4-morpholinophenyl)-2-oxooxazolidin-5-yl)-2-phenylethyl)amino)-1-oxopropan-2-yl)carbamate (9bv)**. White solid, yield 40%. M.p. 123-125 °C. FTIR: 3298, 3063, 2961, 1758, 1726, 1682, 1515, 1229, 1031 cm<sup>-1</sup>. <sup>1</sup>H NMR(400 MHz, CDCl<sub>3</sub>):  $\delta$  7.74 (d,  $J$ =7.6 Hz, 1H), 7.67 (m, 2H), 7.42 (m, 2H), 7.31 (m, 2H), 7.21 (m, 2H), 7.16 (m, 1H), 7.03 (m, 8H), 6.69 (m, 1H), 4.41 (m, 1H), 4.31 (m, 2H), 4.20 (m, 1H), 4.14 (m, 1H), 4.05 (m, 1H), 3.59 (m, 1H), 3.46 (m, 1H), 3.07 (m, 1H), 2.90 (m, 1H). <sup>13</sup>C NMR (100 MHz, CDCl<sub>3</sub>):  $\delta$  172.8, 155.0(d,  $J_{C-F}$ =249.5), 154.7, 154.6, 144.0, 143.9, 143.6, 141.3, 136.6(d,  $J_{C-F}$ =9.0), 136.5, 136.3, 132.5(d,  $J_{C-F}$ =12.0), 130.9, 129.2, 128.8, 128.7, 127.6, 127.1, 127.0, 125.1, 122.7, 119.9, 118.7(d,  $J_{C-F}$ =6.0), 114.1(d,  $J_{C-F}$ =2.0), 107.6(d,  $J_{C-F}$ =26.9), 72.4, 67.0, 66.9, 55.8, 51.0, 50.9, 47.3, 47.0, 42.3, 38.8. MS(ESI): 796 [M+H]<sup>+</sup>.

**(9H-fluoren-9-yl)methyl ((2S)-4-(tert-butoxy)-1-(((S)-1-((R)-3-(3-fluoro-4-morpholinophenyl)-2-oxooxazolidin-5-yl)-2-phenylethyl)amino)-1-oxopentan-2-yl)carbamate (9bw)**. White solid, yield 43%. M.p. 89-91 °C. FTIR: 3304, 3063, 2972, 1756, 1721, 1680, 1514, 1224, 1032 cm<sup>-1</sup>. <sup>1</sup>H NMR (400 MHz, CDCl<sub>3</sub>):  $\delta$  7.75 (d,  $J$ =7.4 Hz, 2H), 7.50 (t,  $J$ =7.5, 2H), 7.39 (t,  $J$ =7.3 Hz, 2H), 7.31 (m, 2H), 7.22-7.07 (m, 5H), 7.01 (m, 1H), 6.88 (m, 1H), 6.71 (m, 2H), 5.39 (brs, 1H), 5.34 (brs, 1H), 4.43 (m, 1H), 4.33 (m, 1H), 4.15 (m, 2H), 3.88 (m, 1H), 3.86 (m, 4H), 3.50 (m, 2H), 3.03 (m, 4H), 2.81 (m, 2H), 1.29 (s, 9H), 1.25 (s, 3H). <sup>13</sup>C NMR (100 MHz, CDCl<sub>3</sub>):  $\delta$  171.5, 154.2, 153.4, 143.7, 141.4, 136.2, 135.6, 129.3, 128.7, 127.8, 127.8, 127.1, 126.9, 124.9, 120.1, 118.6, 114.2 (d,  $J_{C-F}$  = 3 Hz), 107.8 (d,  $J_{C-F}$  = 26 Hz), 72.7, 68.2, 67.1, 66.9, 55.5, 52.2, 51.0, 47.7, 47.1, 37.0, 28.2, 14.7. MS(ESI): 765 [M+H]<sup>+</sup>.

**(9H-fluoren-9-yl)methyl ((S)-1-(((S)-1-((S)-3-(3-fluoro-4-morpholinophenyl)-2-oxooxazolidin-5-yl)ethyl)amino)-1-oxo-3-phenylpropan-2-yl)carbamate (10as)**. White solid, yield 40%. M.p. 105.5-106.5 °C. <sup>1</sup>H NMR (400 MHz, CDCl<sub>3</sub>):  $\delta$  7.70 (d,  $J$  = 7.5 Hz,

2H), 7.41 (t,  $J=7.5$  Hz, 2H), 7.38 (m, 3H), 7.22 (m, 2H), 7.10 (m, 6H), 6.89 (m, 1H), 5.63 (d,  $J=7.5$  Hz, 1H), 4.57 (m, 1H), 4.50 (m, 1H), 4.37 (m, 1H), 4.25 (m, 1H), 4.15 (m, 1H), 4.06 (m, 1H), 3.79 (m, 3H), 3.56 (m, 1H), 2.92 (m, 6H), 1.65 (m, 1H), 1.26 (d,  $J=6.9$  Hz, 3H).  $^{13}\text{C}$  NMR (100 MHz,  $\text{CDCl}_3$ ):  $\delta$  172.3, 155.9, 155.5 (d,  $J_{\text{C-F}}=244.1$  Hz), 154.9, 143.7, 141.2, 136.4 (d,  $J_{\text{C-F}}=8.9$  Hz), 132.9 (d,  $J_{\text{C-F}}=9.2$  Hz), 127.6, 127.0, 125.0, 120.0, 118.8 (d,  $J_{\text{C-F}}=3.7$  Hz), 114.0 (d,  $J_{\text{C-F}}=3.2$  Hz), 107.5 (d,  $J_{\text{C-F}}=26.3$  Hz), 75.2, 67.2, 66.9, 56.2, 50.9, 47.4, 47.1, 46.3, 38.0, 17.2. MS(ESI): 679  $[\text{M}+\text{H}]^+$ , 701  $[\text{M}+\text{Na}]^+$ , 717  $[\text{M}+\text{K}]^+$ .

**(9H-fluoren-9-yl)methyl ((S)-3-(4-(tert-butoxy)phenyl)-1-(((S)-1-((S)-3-(3-fluoro-4-morpholinophenyl)-2-oxooxazolidin-5-yl)ethyl)amino)-1-oxopropan-2-yl)carbamate**

**(10at)**. White solid, yield 40%. M.p. 98.5-99.5 °C  $^1\text{H}$  NMR (400 MHz,  $\text{CDCl}_3$ ):  $\delta$  7.72 (m, 2H), 7.44 (m, 2H), 7.43 (m, 1H), 7.37 (m, 2H), 7.27 (m, 2H), 7.03 (m, 2H), 6.87 (m, 3H), 6.20 (d,  $J=8.6$  Hz, 1H), 4.63 (m, 1H), 4.38 (m, 3H), 4.18 (m, 1H), 4.09 (m, 1H), 3.81 (m, 3H), 3.69 (m, 1H), 2.93 (m, 6H), 1.38 (m, 9H), 1.27 (d,  $J=6.3$  Hz, 3H).  $^{13}\text{C}$  NMR (100 MHz,  $\text{CDCl}_3$ ):  $\delta$  176.8, 155.9, 155.5 (d,  $J_{\text{C-F}}=254.2$  Hz), 154.7, 143.5, 141.2, 136.7 (d,  $J_{\text{C-F}}=8.2$  Hz), 131.7 (d,  $J_{\text{C-F}}=9.3$  Hz), 127.6, 127.0, 125.0, 119.9, 118.7 (d,  $J_{\text{C-F}}=4.4$  Hz), 114.0 (d,  $J_{\text{C-F}}=3.7$  Hz), 107.8 (d,  $J_{\text{C-F}}=30.7$  Hz), 78.5, 74.7, 67.3, 66.9, 54.9, 50.8, 47.3, 47.2, 46.9, 37.2, 28.8, 17.4. MS(ESI): 751  $[\text{M}+\text{H}]^+$ , 773  $[\text{M}+\text{Na}]^+$ , 789  $[\text{M}+\text{K}]^+$ .

**(9H-fluoren-9-yl)methyl ((S)-1-(((S)-1-((S)-3-(3-fluoro-4-morpholinophenyl)-2-oxooxazolidin-5-yl)ethyl)amino)-4-methyl-1-oxopentan-2-yl)carbamate (10au)**. White solid, yield 38 %. M.p. 110.5-111.5 °C  $^1\text{H}$  NMR (400 MHz,  $\text{CDCl}_3$ ):  $\delta$  7.70 (m, 2H), 7.49 (m, 3H), 7.34 (m, 2H), 7.22 (m, 2H), 7.01 (m, 1H), 6.81 (m, 1H), 6.44 (sa, 1H), 4.63 (m, 1H), 4.33 (m, 3H), 4.20 (m, 2H), 3.93 (t,  $J=8.9$  Hz, 1H), 3.82 (m, 4H), 3.78 (m, 1H), 2.96 (m, 4H), 1.73 (m, 2H), 1.59 (m, 1H), 1.31 (d,  $J=5.8$  Hz, 3H), 0.69 (d,  $J=6.2$  Hz, 3H), 0.66 (d,  $J=6.3$  Hz, 3H).  $^{13}\text{C}$  NMR (100 MHz,  $\text{CDCl}_3$ ):  $\delta$  171.0, 156.1, 155.5 (d,  $J_{\text{C-F}}=245.2$  Hz), 154.5, 143.6, 141.2, 136.4 (d,  $J_{\text{C-F}}=7.0$  Hz), 133.0 (d,  $J_{\text{C-F}}=10.0$  Hz), 154.7, 1143.8, 141.2, 127.6, 127.0, 125.0, 119.9, 118.8, 114.0, 107.5 (d,  $J_{\text{C-F}}=26.4$  Hz), 75.9, 67.0, 66.9, 53.6, 50.9, 47.5, 47.0, 46.8, 42.0, 24.6, 22.4, 21.4, 14.5. MS(ESI): 645  $[\text{M}+\text{H}]^+$ , 667  $[\text{M}+\text{Na}]^+$ , 683  $[\text{M}+\text{K}]^+$ .

**(9H-fluoren-9-yl)methyl ((S)-1-(((S)-1-((S)-3-(3-fluoro-4-morpholinophenyl)-2-oxooxazolidin-5-yl)ethyl)amino)-3-(1H-indol-3-yl)-1-oxopropan-2-yl)carbamate (10av)**. White solid, yield 36 %. M.p. 106.5-107.5 °C  $^1\text{H}$  NMR (400 MHz,  $\text{CDCl}_3$ ):  $\delta$  7.75 (t,  $J=9.1$  Hz,

2H), 7.55 (m, 3H), 7.38 (m, 2H), 7.32 (m, 2H), 7.28 (m, 2H), 7.17 (m, 1H), 7.11 (m, 1H), 6.99 (m, 2H), 6.88 (m, 1H), 5.92 (sa, 1 H), 4.43 (m, 3H), 4.19 (t,  $J=8.1$  Hz, 1H), 4.05 (m, 1H), 3.95 (m, 1H), 3.86 (m, 4H), 3.59 (t,  $J=9.0$  Hz, 1H), 3.41 (dd,  $J=9.0, 6.4$  Hz, 1H), 3.29 (m, 1H), 3.15 (m, 1H), 1.00 (m, 3H).  $^{13}\text{C}$  NMR (100 MHz,  $\text{CDCl}_3$ ):  $\delta$  171.2, 155.4 (d,  $J_{\text{C-F}}=252.0$  Hz), 154.3, 154.2, 143.7, 141.3, 137. (d,  $J_{\text{C-F}}=10.3$  Hz), 136.2, 131.0 (d,  $J_{\text{C-F}}=13.9$  Hz), 127.8, 127.2, 127.0, 125.0, 123.4, 122.4, 120.0, 119.9 (d,  $J_{\text{C-F}}=7.4$  Hz), 119.7, 114.0 (d,  $J_{\text{C-F}}=3.2$  Hz), 111.3, 107.5 (d,  $J_{\text{C-F}}=21.8$  Hz), 74.1, 67.1, 66.9, 55.9, 51.0, 47.5, 47.4, 47.1, 28.5, 14.1. MS(ESI):  $[\text{M}+\text{H}]^+=718$  amu,  $[\text{M}+\text{Na}]^+=740$  amu,  $[\text{M}+\text{K}]^+=756$  amu.

**(9H-fluoren-9-yl)methyl ((2S)-3-(tert-butoxy)-1-(((S)-1-((S)-3-(3-fluoro-4-morpholinophenyl)-2-oxooxazolidin-5-yl)ethyl)amino)-1-oxobutan-2-yl)carbamate**

**(10aw).** White solid, yield 41 %. M.p. 80.5-81.5 °C  $^1\text{H}$  NMR (400 MHz,  $\text{CDCl}_3$ ):  $\delta$  7.75 (m, 2H), 7.60 (m, 2H), 7.48 (m, 1H), 7.39 (m, 2H), 7.30 (m, 2H), 7.06 (m, 1H), 6.88 (m, 1H), 5.85 (sa, 1 H), 4.69 (m, 2H), 4.36 (m, 2H), 4.34 (m, 1H), 4.21 (m, 1H), 4.13 (m, 1H), 3.94 (m, 1H), 3.85 (m, 4H), 3.78 (t,  $J=8.1$  Hz, 1H), 3.03 (m, 4H), 1.37 (d,  $J=8.1$  Hz, 3H), 1.26 (s, 9H), 0.85 (d,  $J=6.1$  Hz, 3H).  $^{13}\text{C}$  NMR (100 MHz,  $\text{CDCl}_3$ ):  $\delta$  169.7, 156.0, 155.9, 155.4 (d,  $J_{\text{C-F}}=252.0$  Hz), 143.6, 141.2, 136.1 (d,  $J_{\text{C-F}}=13.0$  Hz), 133.1 (d,  $J_{\text{C-F}}=7.0$  Hz), 127.7, 127.0, 125.0, 120.0, 118.8 (d,  $J_{\text{C-F}}=3.2$  Hz), 113.8 (d,  $J_{\text{C-F}}=2.6$  Hz), 107.7 (d,  $J_{\text{C-F}}=26.4$  Hz), 79.6, 74.9, 67.0, 66.9, 66.2, 55.5, 51.0, 47.4, 47.1, 46.1, 28.2, 27.9, 18.1. MS(ESI): 689  $[\text{M}+\text{H}]^+$ , 711  $[\text{M}+\text{Na}]^+$ , 729  $[\text{M}+\text{K}]^+$ .

**(9H-fluoren-9-yl)methyl ((R)-3-(tert-butylthio)-1-(((S)-1-((S)-3-(3-fluoro-4-morpholinophenyl)-2-oxooxazolidin-5-yl)ethyl)amino)-1-oxopropan-2-yl)carbamate**

**(10ax).** White solid, yield 36 %. M.p. 116.0-117.0 °C.  $^1\text{H}$  NMR ( $\text{CDCl}_3$ , 400 MHz):  $\delta$  7.71 (m, 2H), 7.50 (m, 2H), 7.36 (m, 3H), 7.28 (m, 11H), 7.05 (m, 1H), 6.86 (m, 1H), 4.63 (m, 1H), 4.38 (m, 2H), 4.11 (m, 3H), 3.84 (m, 1H), 3.81 (m, H), 3.76 (m, 1H), 3.01 (m, 1H), 2.93 (m, 4H), 2.80 (m, 1H), 1.20 (s, 3H).  $^{13}\text{C}$  NMR ( $\text{CDCl}_3$ , 100 MHz):  $\delta$  167.0, 155.8 (d,  $J=233.2$  Hz), 155.7, 154.3, 143.5, 141.5, 135.7 (d,  $J=10.0$  Hz), 133.2 (d,  $J=11.1$  Hz), 132.4, 129.5, 128.2, 128.1, 127.6, 127.0, 125.2, 119.8, 118.3 (d,  $J=4.0$  Hz), 114.0, 107.7 (d,  $J=27.8$  Hz), 78.3, 74.8, 68.3, 66.9, 55.7, 50.9, 47.3, 47.0, 46.5, 30.4, 17.0.

**(9H-fluoren-9-yl)methyl ((S)-1-(((S)-1-((S)-3-(3-fluoro-4-morpholinophenyl)-2-oxooxazolidin-5-yl)ethyl)amino)-1-oxo-3-(1-trityl-1H-imidazol-4-yl)propan-2-**

**yl)carbamate (10ay).** White solid, yield 36 %. M.p. 134.5-135.5 °C. FTIR: 3304, 3059, 2955, 1750, 1718, 1671, 1513, 1228, 1114  $\text{cm}^{-1}$ .  $^1\text{H}$  NMR ( $\text{CDCl}_3$ , 400 MHz):  $\delta$  7.67 (m, 3H), 7.50 (m, 3H), 7.30 (m, 5H), 7.22 (m, 9H), 7.00 (m, 7H), 6.77 (dd,  $J=9.5, 8.9$  Hz, 1H), 6.6 (sa, 1H), 4.42 (m, 1H), 4.37 (m, 1H), 4.23 (m, 2H), 4.10 (m, 2H), 3.77 (m, 6H), 2.95 (m, 6H), 1.13 (d,  $J=6.5$  Hz, 3H).  $^{13}\text{C}$  NMR ( $\text{CDCl}_3$ , 100 MHz):  $\delta$  178.3, 155.5 (d,  $J=252.0$  Hz), 155.1, 154.8, 143.5, 141.0, 136.1, 134.0, 133.6, 132.6, 130.9, 129.6, 128.2, 127.8, 127.8, 127.0, 124.9, 124.9, 120.1, 119 (d,  $J=1.6$  Hz), 114.1, 107.7 (d,  $J=27.4$  Hz), 79.4, 73.6, 67.7, 66.9, 54.9, 51.0, 48.0, 47.8, 47.7, 29.6, 17.8. MS(ESI):  $[\text{M}+\text{H}]^+=912$  amu,  $[\text{M}+\text{Na}]^+=934$  amu,  $[\text{M}+\text{K}]^+=950$  amu.

**(9H-fluoren-9-yl)methyl ((S)-3-(tert-butoxy)-1-(((S)-1-((S)-3-(3-fluoro-4-morpholinophenyl)-2-oxooxazolidin-5-yl)ethyl)amino)-1-oxopropan-2-yl)carbamate**

**(10az).** White solid, yield 36 %. M.p. 91.0-92.0 °C. FTIR: 3296, 3020, 2969, 1736, 1715, 1669, 1514, 1225, 1114  $\text{cm}^{-1}$ .  $^1\text{H}$  NMR ( $\text{CDCl}_3$ , 400 MHz):  $\delta$  7.74 (m, 2H), 7.52 (m, 2H), 7.38 (m, 3H), 7.30 (m, 2H), 7.00 (m, 1H), 6.84 (m, 1H), 6.79 (s, 1H), 5.59 (s, 1H), 4.63 (m, 1H), 4.42 (m, 1H), 4.23 (m, 2H), 4.16 (m, 2H), 3.82 (m, 6H), 3.74 (dd,  $J=9.2, 9.1$  Hz, 1H), 3.37 (dd,  $J=8.9, 8.4$  Hz, 1H), 2.97 (m, 4H), 1.36 (d,  $J=6.9$  Hz, 3H).  $^{13}\text{C}$  NMR ( $\text{CDCl}_3$ , 100 MHz):  $\delta$  171.0, 156.5 (d,  $J=225.1$  Hz), 156.1, 154.6, 143.9, 141.2, 136.2 (d,  $J=9.0$  Hz), 133.5 (d,  $J=9.8$  Hz), 127.6, 127.0, 125.0, 119.9, 118.8 (d,  $J=4.5$  Hz), 113.9 (d,  $J=3.5$  Hz), 107.6 (d,  $J=20.0$  Hz), 78.2, 75.2, 68.1, 66.8, 61.5, 56.1, 50.9, 47.4, 47.0, 46.3, 27.3, 17.9. MS(ESI):  $[\text{M}+\text{H}]^+=675$  amu,  $[\text{M}+\text{Na}]^+=697$  amu,  $[\text{M}+\text{K}]^+=713$  amu.

**(9H-fluoren-9-yl)methyl ((S)-1-(((S)-1-((S)-3-(3-fluoro-4-morpholinophenyl)-2-oxooxazolidin-5-yl)-2-phenylethyl)amino)-1-oxo-3-phenylpropan-2-yl)carbamate**

**(10bs).** White solid, yield 45%. M.p. 87-89 °C. FTIR: 3309, 3035, 2960, 1775, 1760, 1684, 1517, 1448, 1221  $\text{cm}^{-1}$ .  $^1\text{H}$  NMR (400 MHz,  $\text{CDCl}_3$ ):  $\delta$  7.72 (d,  $J=7.5$  Hz, 2H), 7.42 (m, 2H), 7.40-7.10 (m, 15H), 7.03 (m, 1H), 6.76 (m, 1H), 5.24 (sa, 1H), 4.62 (d,d,  $J_1=8.2$  Hz,  $J_2=7.7$  Hz, 1H), 4.49 (d,d,  $J_1=9.1$  Hz,  $J_2=9.0$  Hz, 1H), 4.41 (m, 1H), 4.22 (m, 2H), 4.05 (m, 1H), 3.78 (m, 5H), 3.62 (m, 1H), 2.96 (m, 3H), 2.90 (m, 4H), 2.78 (m, 1H).  $^{13}\text{C}$  NMR (100 MHz,  $\text{CDCl}_3$ ):  $\delta$  172.2, 155.6 (d,  $J=244.0$  Hz), 154.1, 153.9, 143.8, 141.2, 136.5, 136.4, 136.1 (d,  $J=8.6$  Hz), 132.5, 130.8, 129.3, 129.0, 49.6, 128.8, 128.6, 127.7, 127.0, 125.1, 124.9, 119.9,

118.6 (d,  $J = 3.8$  Hz), 114.2 (d,  $J = 7.0$  Hz), 107.7 (d,  $J = 26.1$  Hz), 72.5, 66.9, 68.1, 56.5, 51.7, 50.6, 47.3, 38.8, 38.1. MS(ESI): 755 [M+H]<sup>+</sup>.

**(9H-fluoren-9-yl)methyl ((S)-3-(4-(tert-butoxy)phenyl)-1-(((S)-1-((S)-3-(3-fluoro-4-morpholinophenyl)-2-oxooxazolidin-5-yl)-2-phenylethyl)amino)-1-oxopropan-2-yl)carbamate (10bt).** White solid, yield 49 %. M.p. 128-130 °C. FTIR: 3310, 3067, 2978, 1752, 1717, 1670, 1515, 1224, 1046 cm<sup>-1</sup>. <sup>1</sup>H NMR (400 MHz, CDCl<sub>3</sub>): δ 7.72 (d,  $J = 7.5$  Hz, 1H), 7.41 (m, 2H), 7.40-7.20 (m, 5H), 7.39 (m, 1H), 7.26 (m, 1H), 7.01 (m, 1H), 6.95 (d,  $J = 8.0$  Hz, 2H), 6.84 (d,  $J = 8.3$  Hz, 2H), 6.78 (m, 1H), 4.98 (d,  $J = 6.4$  Hz, 1H), 4.63 (dd,  $J_1 = 8.7$  Hz,  $J_2 = 8.2$  Hz, 1H), 4.51 (dd,  $J_1 = 8.5$  Hz,  $J_2 = 8.4$  Hz, 1H), 4.28 (m, 1H), 4.19 (m, 1H), 4.05 (m, 1H), 3.84 (m, 2H), 3.79 (m, 6H), 2.95 (m, 1H), 2.92 (m, 4H), 2.72 (m, 1H), 1.29 (s, 9H). <sup>13</sup>C NMR (100 MHz, CDCl<sub>3</sub>): δ 176.7, 156.6, 154.6 (d,  $J = 244.0$  Hz), 154.7, 154.3, 143.8, 141.2, 139.0, 136.5, 135.4, 132.5, 129.9, 129.4, 129.2, 128.8, 127.6, 127.1, 127.0, 125.0, 124.3, 118.7 (d,  $J = 2.9$  Hz), 114.1 (d,  $J = 3.6$  Hz), 107.7 (d,  $J = 26.0$ ), 78.4, 72.4, 67.3, 66.9, 56.6, 51.4, 51.0, 47.3, 46.9, 38.0, 37.1, 28.8, MS(ESI): 414 [2M+2H]/2<sup>+</sup>.

**(9H-fluoren-9-yl)methyl ((S)-1-(((S)-1-((S)-3-(3-fluoro-4-morpholinophenyl)-2-oxooxazolidin-5-yl)-2-phenylethyl)amino)-4-methyl-1-oxopentan-2-yl)carbamate (10bu).** White solid, yield 40%. M.p. 68-70 °C. FTIR: 3305, 3064, 2959, 1757, 1715, 1686, 1516, 1225, 1031 cm<sup>-1</sup>. <sup>1</sup>H NMR (400 MHz, CDCl<sub>3</sub>): δ 7.73 (d,  $J = 7.6$  Hz, 1H), 7.56 (d,  $J = 7.5$  Hz), 7.53 (m, 2H), 7.52 (m, 1H), 7.45 (d,  $J = 14.0$  Hz, 1H), 7.37 (t,  $J = 7.5$  Hz, 1H), 7.27 (t,  $J = 7.5$  Hz, 1H), 7.17 (m, 2H), 7.03 (m, 1H), 6.80 (m, 1H), 5.22 (sa, 1H), 4.70 (d,  $J_1 = 8.5$  Hz,  $J_2 = 7.7$  Hz, 1H), 4.55 (d,  $J_1 = 8.5$  Hz,  $J_2 = 8.4$  Hz, 1H), 4.24 (m, 1H), 4.17 (m, 2H), 4.10 (t,  $J = 7.2$ , 1H), 3.83 (m, 1H), 3.81 (m, 4H), 3.74 (m, 1H), 2.99 (d,  $J = 8.1$  Hz, 2H), 2.94 (m, 4H), 1.42 (m, 1H), 1.31 (m, 2H), 0.92 (s, 6H). <sup>13</sup>C NMR (100 MHz, CDCl<sub>3</sub>): δ 167.8, 155.6 (d,  $J = 244.0$  Hz), 154.5, 154.0, 143.9, 141.3, 136.6, 136.4 (d,  $J = 8.7$  Hz), 132.5 (d,  $J = 10.0$  Hz), 130.9, 127.7, 127.0, 126.9, 125.1, 125.0, 119.9, 118.2 (d,  $J = 2.9$  Hz), 114.2 (d,  $J = 3.6$  Hz), 107.3 (d,  $J = 24.0$  Hz), 72.5, 68.2, 67.0, 53.9, 52.0, 51.0, 47.3, 47.1, 41.7, 37.9, 24.8, 22.9. MS(ESI): 721 [M+H]<sup>+</sup>.

**(9H-fluoren-9-yl)methyl ((S)-1-(((S)-1-((S)-3-(3-fluoro-4-morpholinophenyl)-2-oxooxazolidin-5-yl)-2-phenylethyl)amino)-3-(2H-indol-3-yl)-1-oxopropan-2-yl)carbamate (10bv).** White solid, yield 43%. M.p. 121-123 °C. FTIR: 3298, 3063, 2961,

1758, 1726, 1682, 1515, 1229, 1031  $\text{cm}^{-1}$ .  $^1\text{H}$  NMR (400 MHz,  $\text{CDCl}_3$ ):  $\delta$  7.72 (d,  $J=7.6$  Hz, 1H), 7.37-7.13 (m, 11H), 7.37 (t,  $J=7.0$  Hz, 1H), 7.45 (m, 1H), 7.44 (d,  $J=7.5$  Hz, 1H), 7.28 (t,  $J=9.0$  Hz, 1H), 7.01 (m, 1H), 6.81 (m, 1H), 5.30 (sa, 1H), 4.53 (d,d  $J_1=8.5$  Hz,  $J_2=7.7$  Hz, 1H), 4.45 ((d,d  $J_1=8.5$  Hz,  $J_2=8.4$  Hz, 1H), 4.25 (m, 2H), 4.19 (m, 1H), 4.09 (m, 1H), 3.82 (m, 4H), 3.14 (m, 2H), 3.05 (d,d  $J_1=14.6$  Hz,  $J_2=7.2$  Hz, 2H), 2.97 (m, 4H), 2.81 (m, 1H), 2.79 (m, 1H).  $^{13}\text{C}$  NMR(100 MHz,  $\text{CDCl}_3$ ):  $\delta$  172.8, 155.0 (d,  $J=249.5$  Hz), 154.7, 154.0, 144.0, 143.9, 143.6, 141.3, 136.6 (d,  $J=9.0$  Hz), 136.5, 136.3, 132.5 (d,  $J=12.0$  Hz), 130.9, 129.2, 128.8, 128.7, 127.7, 127.1, 127.0, 125.1, 122.7, 119.9, 118.7 (d,  $J=6.0$  Hz), 114.1 (d,  $J=2.0$ ), 107.6 (d,  $J=26.9$  Hz), 72.4, 67.0, 66.9, 55.8, 51.0, 50.9, 47.3, 47.0, 42.3, 38.8. MS(ESI): 795  $[\text{M}]^+$ .

**(9H-fluoren-9-yl)methyl ((2S)-3-(tert-butoxy)-1-(((S)-1-((S)-3-(3-fluoro-4-morpholinophenyl)-2-oxooxazolidin-5-yl)-2-phenylethyl)amino)-1-oxobutan-2-yl)carbamate (10bw)**. White solid, yield 40%. M.p. 89-91  $^\circ\text{C}$ . FTIR: 3304, 3063, 2972, 1756, 1721, 1680, 1514, 1224, 1032  $\text{cm}^{-1}$ . NMR  $^1\text{H}$  (400 MHz,  $\text{CDCl}_3$ ):  $\delta$  3.87 (m, 1H), 3.78 (m, 1H), 7.74 (d,  $J=7.6$  Hz, 1H), 7.56 (d,  $J=7.4$  Hz, 1H), 7.45 (m, 1H), 7.38 (t,  $J=7.5$  Hz, 1H), 7.34 (m, 2H), 7.31 (t,  $J=7.0$  Hz, 1H), 7.30 (m, 1H), 7.28 (m, 2H), 7.02 (d,  $J=8.1$  Hz, 1H), 6.87 (d,  $J=9.1$ , 1H), 5.84 (sa, 1H), 4.67 (d,d  $J_1=8.5$  Hz,  $J_2=7.8$  Hz, 1H), 4.51 (d,d  $J_1=8.5$  Hz,  $J_2=8.4$  Hz, 1H), 4.33 (d,  $J=7.0$ , 2H), 4.20 (m, 1H), 4.11 (m, 1H), 4.08 (m, 1H), 3.85 (m, 4H), 3.02 (m, 4H), 3.01 (m, 2H), 2.04 (s, 3H), 1.23 (s, 9H).  $^{13}\text{C}$  NMR (100 MHz,  $\text{CDCl}_3$ ):  $\delta$  170.1, 155.7 (d,  $J=240.0$  Hz), 154.2, 153.9, 143.6, 141.3, 136.5, 136.3 (d,  $J=9.0$  Hz), 133.1 (d,  $J=10.3$  Hz), 129.3, 128.9, 127.7, 127.1, 127.1, 125.1, 119.9, 118.7 (d,  $J=2.8$  Hz), 113.8 (d,  $J=3.8$  Hz), 107.5 (d,  $J=26.0$  Hz), 67.0, 75.8, 72.0, 67.0, 66.1, 59.0, 51.9, 51.0, 47.2, 47.1, 38.5, 28.1, 14.2. MS(ESI): 765  $[\text{M}]^+$ .

### 5.3. Antimicrobial activity

The antibacterial activity of all molecules was evaluated against ATCC bacteria strain both Gram-positive (*S. aureus*, *E. faecalis* and MRSA) and Gram-negative (*E. coli*), also seven clinical isolates (*Streptococcus grupo A-4*, *Staphylococcus aureus 05*, *Salmonella thypi 13*, *Escherichia coli 09*, MRSA-03, MRSA-04 and MRSA-05) were tested.<sup>49-51</sup> All bacteria were cultured in Muller-Hinton broth. MIC of all compounds were determined by broth microdilution method according to CLSI guidelines. The 18-20 h grown culture gives

about  $10^8$  CFU/mL of bacteria. The bacterial cultures were diluted to give approximately  $10^6$  CFU/mL in Muller-Hinton broth media and then were used to determinate antibacterial efficacy.

The evaluation of the antibacterial activity of compounds against different gram-positive and gram-negative strains at a single concentration of 50  $\mu\text{g/mL}$  was performed. Six compounds (**10as**, **10ay**, **9as**, **9ay**, **9ax** and derivatives of alanine and **9bu** of phenylalanine) showed activity at this concentration against the *Streptococcus* group A strain. Subsequently, to these compounds, they were determined the minimum inhibitory concentration (MIC) evaluated at different dilutions of 25.0-0.38  $\mu\text{g/mL}$ .

#### 5.4. *Mycobacterium tuberculosis* activity

**Strains.** Three strains of *M. tuberculosis* clinical isolates from the General Hospital of Tijuana, Baja California, Mexico were selected. These strains exhibit resistance to rifampicin, isoniazid, ethambutol and streptomycin and susceptibility to linezolid.

**Absolute concentrations method.** The linezolid susceptibility was determined for the absolute concentrations method.

**MGIT 960 system.** Each clinical isolate was inoculated into tubes of the MGIT 960 system by testing a series of dilutions of 2.5 to 125 mg/mL of the compounds and of linezolid (Pfizer, NY). To each tube was added 400  $\mu\text{L}$  of PANTA enrichment broth and 200  $\mu\text{L}$  of a solution prepared from each of the compounds with the following concentrations 125, 100, 80, 40, 20, 10, 5, 2.5  $\mu\text{g/L}$ . The tubes were inoculated with 300  $\mu\text{L}$  of suspension of the bacterial strain in 4100  $\mu\text{L}$  of medium of Middlebrook 7H9, to obtain equal concentrations in each tube. The growth control tube was inoculated with the solvent that was used to prepare the solutions of the compounds (DMSO). The growth of the bacteria in the tubes was continuously monitored.

#### 5.5. *Molecular coupling studies (docking).*

The automated molecular coupling studies of 64 linezolid analogues structures were performed with the crystallographic structure of ribosomal RNA of *E.coli* with the use of the MOE 2018 program.

### 5.6. Cellular viability assay

To evaluate the effect of the linezolid analogues (10as, 10ay, 9as, 9ay, 9aw, 9ax and 9bu) on cell proliferation, the human retinal pigment epithelial cell line ARPE-19 was used. The effect of synthesized analogues was determined by MTT assays with some modifications.<sup>47,48</sup> Cells ( $1 \times 10^4$  per well, 50  $\mu$ L) were placed in each well of a 96-well plate (Costar<sup>®</sup>, USA). After 24 h of incubation at 37°C in a 5% CO<sub>2</sub> atmosphere to allow cell attachment, aliquots (50  $\mu$ L) of the medium containing different concentrations of linezolid analogues (100, 50, 25 and 12.5  $\mu$ M) were added. All linezolid analogues were dissolved in dimethyl sulfoxide (DMSO) and subsequently diluted in the culture medium. Doxorubicin was used as a positive control of cytotoxicity in cell viability assays. Cells were treated for 48 h, during the last 4 h of incubation, culture medium was removed, and cells were washed with PBS, afterwards, 10  $\mu$ L of an MTT solution (5 mg/mL) were added to each well. The cell viability was assessed by the ability of metabolically active cells to reduce tetrazolium salt to coloured formazan compounds. The formazan crystals were dissolved with acidic isopropyl alcohol (0.3 %). The sample absorbance was measured on a microplate reader (Multiskan EX, ThermoLabSystem) using a test wavelength of 570 nm and a reference wavelength 650 nm. The effect over cell viability of linezolid analogues was reported as a proliferation percentage, in comparison with DMSO control.

### Acknowledgements

The authors thank to Consejo Nacional de Ciencia y Tecnología (CONACYT) for the financial support through the Research Grant SALUD-2015-1-261324, the Supramolecular Chemistry Thematic Network Grant No. 294810, the ITT NMR facilities Grant INFR-2011-3-173395 and the Scholarship Program, which supported to G. D. García-Olaiz and Eleazar Alcántar-Zavala for their postgraduate studies. The docking software MOE was support by the Instituto de Investigaciones Biomédicas at the UNAM, through the program “Novel alternatives for the Treatment of Infection Diseases (NUATEI-IIB-UNAM)” and the program “Apoyo a la Investigación y el Posgrado (PAIP)” Grant 5000-9163 in the Chemistry Faculty of the UNAM. We also thanks to Samuel Ruvalcaba-Ruiz for the microbiological technical support.

## References

1. Alós, Juan-Ignacio. Resistencia bacteriana a los antibióticos: una crisis global. *Enferm. Infecc. Microbiol. Clin.* **2015**, 33, 692-699. DOI: 10.1016/j.eimc.2014.10.004
2. Centers for Disease Control and Prevention. Antibiotic Resistant Threats in the United States, 2013. Available from: <http://www.cdc.gov/drugresistance/threat-report-2013/pdf/ar-threats-2013-508.pdf>. [Last accessed in July 02, 2019].
3. World Health Organization. WHO Publishes List of Bacteria for Which New Antibiotics are Urgently Needed; 2017. Available from: <https://www.who.int/news-room/detail/27-02-2017-who-publishes-list-of-bacteria-for-which-new-antibiotics-are-urgently-needed>. [Last accessed in July 02, 2019].
4. Pigrau, C.; Almirante, B. Oxazolidinonas, glucopéptidos y lipopéptidos cíclicos. *Enferm. Infecc. Microbiol. Clin.* **2009**, 27, 236-246. DOI: 10.1016/j.eimc.2009.02.004
5. Gomez-Gener, A.; Salvador, M.; Boj, M. Linezolid: una nueva alternativa en infecciones por gram positivos. *Farm. Hosp.* **2002**, 26, 44-48. DOI: 1130-6343/2002/26/01/44.
6. Ippolito, A. J.; Kanyo, F. Z.; Wang, D.; Franceschi, J. F.; Moore, B. P.; Steitz, A. T; Duffy, M. E. Crystal structure of the oxazolidinone antibiotic Linezolid bound to the 50S ribosomal subunit. *J. Med. Chem.* **2008**, 51, 3353-3356. DOI: 10.1021/jm800379d.
7. Saager, B.; Rohde, H.; Timmerbeil, B. S. Molecular characterization of Linezolid resistance in two vancomycin-resistant (VanB) *Enterococcus faecium* isolates using pyrosequencing. *Eur. J. Clin. Microbiol. Infect. Dis.* **2008**; 27, 873-878. DOI: 10.1007/s10096-008-0514-6.
8. Besier, S.; Ludwig, A.; Zander, J.; Brade, V.; Wichelhaus, TA. Linezolid resistance in *Staphylococcus aureus*: gene dosage effect, stability, fitness costs, and cross-resistances. *Antimicrob. Agents. Chemoter.* **2008**, 52, 1570-1572. DOI: 10.1128/AAC.01098-07.

9. Shiau, T.; Turtle, E.; Francavilla, C.; Alvarez, N.; Zuck, M.; Friedman, L.; O'Mahony, D.; Low, E.; Anderson, M.; Najafi, R.; Jain, R. Novel 3-chlorooxazolidin-2-ones as antimicrobial agents. *Bioorg. Med. Chem.* **2011**, *21*, 3025-3028. DOI: 10.1016/j.bmcl.2011.03.036.
10. Rakesh; Sun, D.; Lee, R.; Tangallapally, R.; Lee, R. Synthesis, optimization and structure-activity relationships of 3,5-disubstituted isoxazolines as new anti-tuberculosis agents. *Eur. J. Med. Chem.* **2009**, *44*, 460-472. DOI: 10.1016/j.ejmech.2008.04.007
11. Renslo, A.; Luehr, G.; Lam, S.; Westlund, N.; Gómez, M.; Hackbarth, C.; Patel, D.; Gordeev, M. Synthesis and structure-activity studies of antibacterial oxazolidinones containing dihydrothiopyran or dihydrothiazine C-rings. *Bioorg. Med. Chem. Lett.* **2006**, *16*, 3475-3478. DOI: 10.1016/j.bmcl.2006.03.104
12. Piccionello, A.; Musumeci, R.; Cocuzza, C; Fortuna, C.; Guarcello, A.; Pierro, P.; Pace, A. Synthesis and preliminary antibacterial evaluation of Linezolid-like 1,2,4-oxadiazole derivatives. *Eur. J. Med. Chem.* **2012**, *50*, 441-448. DOI: 10.1016/j.ejmech.2012.02.002
13. <http://www.scribd.com/doc/3760720/Pfizer-RD-Pipeline-as-of-February-2008>.
14. Selva kumar, N.; Govinda Rajulu, G.; Chandra Shekar Reddy, K.; Chandra Chary, B.; Kumar Kalyan, P.; Madhavi, T.; Praveena, K.; Hari Prasada Reddy, K.; Takhi, M.; Mallick, A.; Amarnath, P. V. S.; Kandepu, S.; Iqbal, J. Synthesis, SAR, and antibacterial activity of novel oxazolidinone analogues possessing urea functionality. *Bioorg. Med. Chem. Lett.* **2008**, *18*, 856-860. DOI: 10.1016/j.bmcl.2007.09.024
15. Gravestock, M. B.; Acton, D. G.; Betts, M. J.; Dennis, M.; Hatter, G.; McGregor, A.; Swain, L.; Wilson, R. G.; Woods, L.; Wookey, A. New classes of antibacterial oxazolidinones with C-5, methylene O-Linked heterocyclic side chains. *Bioorg. Med. Chem. Lett.* **2003**, *13*, 4179-4186. DOI: 10.1016/j.bmcl.2003.07.033

16. Rakesh; Sun, D.; Lee, R.; Tangallapally, R.; Lee, R. Synthesis, optimization and structure-activity relationships of 3,5-disubstituted isoxazolines as new anti-tuberculosis agents. *Eur. J. Med. Chem.* **2009**, *44*, 460-472. DOI: 10.1016/j.ejmech.2008.04.007
17. Michalska, K.; Karpiuk, I.; Król, M.; Tyski, S. Recent development of potent analogues of oxazolidinone antibacterials agents. *Bioorg. Med. Chem.* **2013**, *21*, 577-591. DOI: 10.1016/j.bmc.2012.11.036.
18. Varshney, V.; Mishra, N.; Shukla, P.; Sahu, D. Novel 4-N-substituted aryl but-3-ene-1,2-dione derivatives of piperazinyloxazolidinones as antibacterial agents. *Bioorg. Med. Chem. Lett.* **2009**, *19*, 6810-6812. DOI: 10.1016/j.bmcl.2009.07.106
19. Liu, J.; He, B.; Yu, A.; Zhou, W. Synthesis and *in vitro* evaluation of substituted phenyl-piperazinyl-phenyl oxazolidinones against Gram-positive bacteria. *Chem. Biol. Drug. Des.* **2007**, *69*, 265-268. DOI: 10.1111/j.1747-0285.2007.00498.x
20. Paul-Satyaseela, M.; Solanki, S.; Sathishkumar, D.; Bharani, T.; Magesh, V.; Rajagopal, S. *In vitro* antibacterial activities of a novel oxazolidinone, OCID0050. *J. Antimicrob. Chemoter.* **2009**, *64*, 797-800. DOI: 10.1093/jac/dkp300
21. Gadekar, P.; Roychowdhury, A.; Kharkar, P.; Khedkar, V.; Arkile, M.; Manek, H.; Sarkar, D.; Sharma, R.; Vijayakumar, V.; Sarveswari, S. Design, synthesis and biological evaluation of novel azaspiro analogs of linezolid as antibacterial and antitubercular agents. *Eur. J. Chem. Med.* **2016**, *122*, 475-487. DOI: 10.1016/j.ejmech.2016.07.001
22. Bharath, Y.; Alugubelli, G. R.; Sreenivasulu, R.; Rao, M. V. Design, synthesis of novel oxazolidino-amides/sulfonamides conjugates and their impact on antibacterial activity. *Chem. Pap.*; **2017**. DOI: 10.1007/s11696-017-0298-1
23. Craik, D.; Fairlie, D.; Liras, S.; Price, D. The future of peptide based drugs. *Chem. Biol. Drug. Des.* **2013**, *81*, 136-147. DOI: 10.1111/cbdd.12055

24. Huang, X.; Wang, M.; Wang, H.; Chen, Z.; Zhang, Y.; Pan, Y. Synthesis and antitumor activities of novel dipeptide derivatives derived from dehydroabiatic acid. *Bioorg. Med. Chem. Lett.* **2014**, *24*, 1511-1518. DOI: 10.1016/j.bmcl.2014.02.001
25. Sato, K.; Hendricks, M.; Palmer, L.; Stupp, S. Peptide supramolecular materials for therapeutics. *Chem. Soc. Rev.* **2018**, *47*, 7539-7551.
26. Shaw, K. J.; Poppe, S.; Schaadt, R.; Brown-Driver, V.; Finn, J.; Pillar, C. M.; Shinabarger, D.; Zurenko, G. In Vitro activity of TR-700, the antibacterial moiety of the produg TR-701, against Linezolid-resistant strains. *Antimicrob. Agents. Chemother.* **2008**, *52*, 4442-4447. DOI: 10.1128/AAC.00859-08
27. Bai, P.; Qin, S.; Chu, W.; Yang, Y.; Cui, D.; Hua, Y.; Yang, Q.; Zhang, E. Synthesis and antibacterial bioactivities of cationic deacetyl linezolid amphiphiles. *Eur. J. Med. Chem.* **2018**, *155*, 925-945. DOI: 10.1016/j.ejmech.2018.06.054
28. Kline, T.; Felise, H. B.; Barry, C. K.; Jackson, S. T.; Naguyem, H. V.; Miller, S. I. Substituted 2-Imino-5-arylidene-thiazolidin-4-one Inhibitors of Bacterial Type III Secretion. *J. Med. Chem.* **2008**, *51*, 7065-7074. DOI: 10.1021/jm8004515
29. Ochoa-Terán, A.; Rivero, I. Synthesis of enantiopure 1, 3-oxazolidin-2-ones from  $\alpha$ -dibenzilamino esters. *Arkivoc* **2008**, *14*, 330-343. DOI: 10.3998/ark.5550190.0009.e30
30. Córdova-Guerrero, J.; Hernández-Guevara, E.; Ramírez-Zatarain, S.; Núñez-Bautista, M.; Ochoa-Terán, A.; Muñiz-Salazar, R.; Montes-Ávila, J.; López-Angulo, G.; Paniagua-Michel, A.; Nuño Torres, G. A. Antibacterial activity of new oxazolidin-2-one analogues in methicillin-resistant *staphylococcus aureus* strains. *Int. J. Mol. Sci.* **2014**, *15*, 5277-5291. DOI: 10.3390/ijms15045277.
31. Steven, J.; Brickner, S.; Hutchinson, D.; Barbachyn, M.; Mannimen, P.; Ulanowicz, D.; Garmon, S.; Grega, K.; Hedges, S.; Toops, D.; Ford, C.; Zurenko, G. Synthesis and antibacterial activity of U-100592 and U-100766, two oxazolidinone antibacterial agents for

the potential treatment of multidrug-resistant gram-positive bacterial infections. *J. Med. Chem.* **1996**, *39*, 673-679. DOI:10.1021/jm9509556

32. Schuwirth, B.S., Borovinskaya, M.A., Hau, C.W., Zhang, W., Vila-Sanjurjo, A., Holton, J.M., Cate, J.H. Crystal structure of the bacterial ribosome from *Escherichia coli* at 3.5 Å resolution. *Science* **2005**, *310*, 827-834. DOI: 10.1126/science.1117230

33. Molecular Operating Environment (MOE), version 2018.01, Chemical Computing Group Inc., Montreal, Quebec, Canada. Available in <http://www.chemcomp.com>

34. Grunenberg, J.; Licari, G. Effective in silico prediction of new oxazolidinone antibiotics: force field simulations of the antibiotic-ribosome complex supervised by experiment and electronic structure methods. *Beilstein J. Org. Chem.* **2016**, *12*, 415-428. DOI: 10.3762/bjoc.12.45

35. Zhang, N. & Zhao, H. Enriching screening libraries with bioactive fragment space. *Bioorg. Med. Chem. Lett.* **2016**, *26*, 3594-3597. DOI: 10.1016/j.bmcl.2016.06.013

36. Uma. K.; Lalithanba, H.; Chandramohan, V.; Lingaraju, K. A facile synthesis of hydroxamic acids of *N*-protected amino acids employing BDMS, a study of their molecular docking and their antibacterial activities. *Org. Prep. Proced. Int.* **2019**, *51*, 161-174. DOI: 10.1080/00304948.2019.1579039

37. Morán-Ramallal, R.; Liz, R.; Gotor, V. Regioselective and Stereospecific Synthesis of Enantiopure 1,3-Oxazolidin-2-ones by Intramolecular Ring Opening of 2-(Boc-aminomethyl)aziridines. Preparation of the antibiotic Linezolid. *Org. Lett.* **2008**, *10*, 1935-1938. DOI: 10.1021/ol800443p

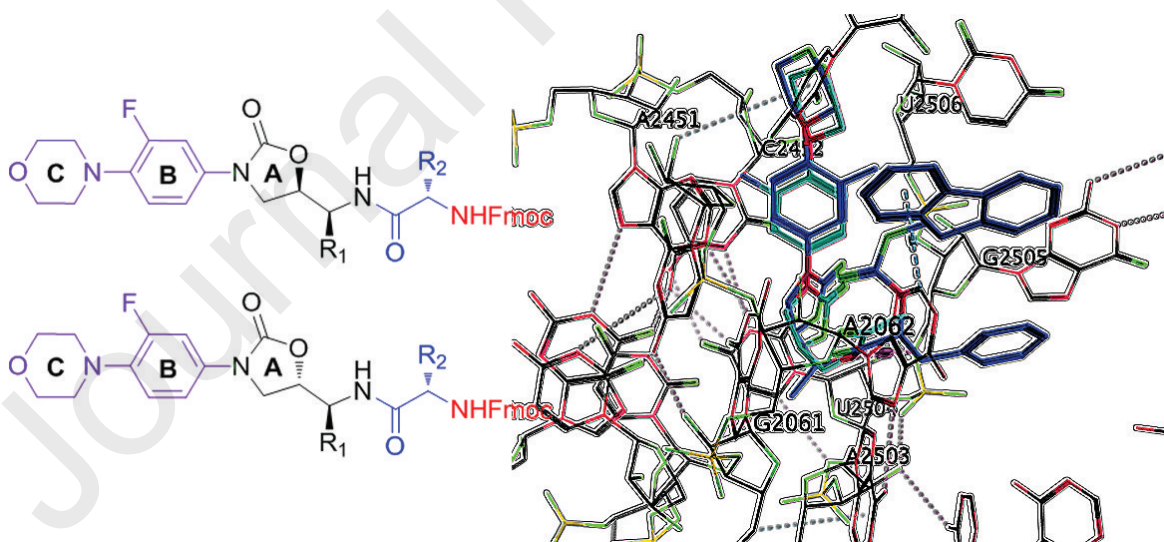
38. Reetz, M. T.; Drewes, M. W.; Harms, K.; Reif, W. Stereoselective cyanohydrin-forming reactions of chiral  $\alpha$ -amino aldehydes. *Tetrahedron Lett.* 1988, *29*, 3295-3298. DOI: 10.1016/0040-4039(88)85144-X.

39. Reetz, M. T. New approaches to the use of amino acids as chiral building blocks in organic synthesis. *Angew. Chem. Int. Ed. Engl.* **1991**, *30*, 1531-1546. DOI: 10.1002/anie.199115313.
40. Reetz, M. T. Metal, ligand and protective group tuning as a means to control selectivity. *Pure Appl. Chem.* **1992**, *64*, 351-359. DOI: 10.1351/pac1992264030351.
41. Reetz, M. T. Synthesis and diastereoselective reactions of *N,N*-dibenzylamino aldehydes and related compounds. *Chem. Rev.* **1999**, *99*, 1121-1162. DOI: 10.1021/cr980417b.
42. Lipinski, C. A.; Lombardo, F.; Dominy, B. W.; Feeney, P. J. Experimental and computational approaches to estimate solubility and permeability in drug discovery and development settings. *Adv. Drug Deliv. Rev.* **2001**, *46*, 3-26. DOI: 10.1016/S0169-409X(00)00129-0.
43. Lipinski, C. A. Lead- and drug-like compounds: the rule-of-five revolution. *Drug Discovery Today: Technologies* **2004**, *1*, 337-341. DOI: 10.1016/j.ddtec.2004.11.007
44. Gülçin, I.; Oktay, M.; Kirecci, E.; Küfrevioğlu, Ö. Screening of antioxidant and antimicrobial activities of anise (*Pimpinella anisum* L.) seed extracts. *Food Chem.* **2003**, *83*, 371-382. DOI:10.1016/S0308-8146(03)00098-0
45. Gülçin, I.; Küfrevioğlu, Ö.; Oktay, M.; Büyükokuroğlu, M. Antioxidant, antimicrobial, antiulcer and analgesic activities of nettle (*Urtica dioica* L.). *J. Ethnopharmacol.* **2004**, *90*, 205-215. DOI:10.1016/j.jep.2003.09.028
46. Gulcin, I.; Tel, A.; Kirecci, E. Antioxidant, antimicrobial, antifungal, and antiradical activities of cyclotrichium niveum (BOISS.) Manden and scheng. *Int. J. Food Prop.* **2008**, *11*, 450-471. DOI:10.1080/10942910701567364

47. Mosmann, T. Rapid colorimetric assay for cellular growth and survival: application to proliferation and cytotoxicity assays. *J. Immunol. Methods.* **1983**, *65*, 55-63. DOI:10.1016/0022-1759(83)90303-4.
48. Hernandez, J.; Goycoolea, F.; Quintero, J.; Acosta, A.; Castañeda, M.; Dominguez, Z.; Robles, R.; Vazquez-Moreno, L.; Velazquez, E.; Astiazaran, H.; Lugo, E.; Velazquez, C. Sonoran propolis: chemical composition and antiproliferative activity on cancer cell lines. *Planta med.* **2007**, *73*, 1469-1474. DOI: 10.1055/s-2007-990244
49. Tohma, H.; Köksal, E.; Kilic, Ö.; Alan, Y.; Yilmaz, M.; Gülçin, I.; Bursal, E.; Alwasel, S. RP-HPLC/MS/MS Analysis of the phenolic compounds, antioxidant and antimicrobial activities of Salvia L. Species. *Antioxidants* **2016**, *5*, 38. DOI:10.3390/antiox5040038
50. Gülçin, I.; Kirecci, E.; Akkemik, E.; Topal, F.; Hisar, O. Turk. Antioxidant, antibacterial, and anticandidal activities of an aquatic plant: duckweed (*Lemna minor* L. *Lemnaceae*). *J. Biol.* **2010**, *34*, 175-188. DOI: 10.1016/j.bioorg.2016.12.001
51. Kocyigit, U.; Budak, Y.; Gürdere, M.; Tekin, S.; Köprülü, T.; Ertürk, F.; Özcan, K.; Gülçin, I.; Ceylan, M. Synthesis, characterization, anticancer, antimicrobial and carbonic anhydrase inhibition profiles of novel (3a*R*,4*S*,7*R*,7a*S*)-2-(4-((*E*)-3-(3-aryl)acryloyl)phenyl)-3a,4,7,7a-tetrahydro-1*H*-4,7-methanoisindole-1,3(2*H*)-dione derivatives. *Bioorg. Chem.* **2017**, *70*, 118-125. DOI: 10.1016/j.bioorg.2016.12.001.

## Highlights

- A stereoselective synthesis of 26-Linezolid dipeptide-type analogous was performed.
- The docking analysis shows the favorable couplings of the Linezolid dipeptide-type analogous in the PTS through different type of supramolecular interactions.
- The Linezolid dipeptide-type analogous present antibacterial activity against *S. aureus* and *M. tuberculosis* clinical isolates.
- The active Linezolid dipeptide-type analogous preserve the cellular viability of ARPE-19 cells.



**Declaration of interests**

The authors declare that they have no known competing financial interests or personal relationships that could have appeared to influence the work reported in this paper.

The authors declare the following financial interests/personal relationships which may be considered as potential competing interests: